Basin Research (1996) **8,** 199–223

Interactions of growing folds and coeval depositional systems

Douglas Burbank, Andrew Meigs and Nicholas Brozović

Department of Earth Sciences, University of Southern California, Los Angeles, CA 90089–0740, USA

ABSTRACT

Responses of both modern and ancient fluvial depositional systems to growing folds can be interpreted in terms of interactions among competing controlling variables which can be incorporated into simple conceptual models. The ratio of the rate of sediment accumulation to the rate of structural uplift determines whether a fold develops a topographic expression above local base level. The balance between (a) stream power and rates of upstream deposition vs. (b) bedrock resistance and rates of crestal uplift and of fold widening determines whether an antecedent stream maintains its course or is defeated by a growing structure. Modern drainage configurations in actively folding landscapes can often be interpreted in terms of these competing variables, and through analysis of digital topography, detailed topographic characteristics of these folds can be quantified. Modern examples of growing folds display both defeated and persistent antecedent rivers, deflected drainages and laterally propagating structures. The topography associated with a defeated antecedent river at Wheeler Ridge, California, is consistent with a model in which defeat results from forced aggradation in the piggyback basin, without the need to vary discharge or uplift rate.

Reconstruction of the long-term interplay between a depositional system and evolving folds requires a stratigraphic perspective, such as that provided by syntectonic strata which are directly juxtaposed with ancient folds and faults. Analysis of Palaeogene growth strata bounding the Catalan Coastal Ranges of NE Spain demonstrates the synchronous growth and the kinematic history of multiple folds and faults in the proximal foreland basin. Although dominated by transverse rivers which crossed fold crests, palaeovalleys, interfan lows, structural re-entrants and saddles, and rising anticlines diverted flow and influenced local deposition. In the ancient record, drainage-network events, such as avulsion or defeat of a transverse stream, usually cannot be unambiguously attributed to a single cause. Examination of ancient syntectonic strata from a geomorphological perspective, however, permits successive reconstructions of synorogenic topography, landscapes and depositional systems.

INTRODUCTION

As structural disruption encroaches on the fringes of a terrestrial sedimentary basin, pre-existing patterns of erosion, sediment deposition and transport are perturbed. River systems respond to changes in both local base levels and topography that are imposed by discrete domains of differential uplift and subsidence. This paper focuses primarily on the interplay between the structural evolution of fold-and-thrust belts and patterns of deposition and erosion within deforming foreland basins. We develop a conceptual basis for interpretation of the geomorphological, stratigraphic and structural record of the interactions between terrestrial depositional systems and both growing folds and active faults. Through examination of both modern and ancient examples we explore a variety of depositional geometries that result from fluvial interactions with growing folds. Four variables act as first-order controls on these interactions: (1) characteristics of the fluvial system; (2) the geometry and rates of growth of individual folds and faults; (3) the three-dimensional development of multiple structures; and (4) pre-existing or inherited topography. The response of the fluvial system is strongly influenced by stream power, rates of aggradation and erosion, and pre-existing topography, whereas the surface expression of folds is a function of rates of crestal uplift, substrate resistance and fold geometry. Interactions and feedbacks among these competing variables determine fluvial patterns within actively deforming landscapes. Whereas present-day geomorphology can illustrate some of these interactions, the ancient stratigraphic and structural record provides a view of depositional systems that evolve as the controlling variables change through time.

CONCEPTUAL BASIS FOR RECONSTRUCTING DEPOSITIONAL SYSTEMS AND GROWING FOLDS

In many foreland basins, growing folds result from horizontal shortening and subsequent hangingwall uplift above thrusts that are actively propagating into the basin fill. Folds can also develop due to buckling above shallowly dipping decollements. In this paper, when describing interactions of fluvial systems with growing folds, we do not discriminate among the various types of folds, except when observable stratigraphic geometries are specifically tied to a structural style. Unless otherwise stated, we assume that faults display a vergence toward the foreland, such that an upright fold's backlimb dips toward the hinterland and its forelimb dips toward the foreland. We do differentiate between 'pretectonic' strata which were deposited prior to the deformation described here and 'syntectonic' or 'growth' strata that are coeval with that deformation (Suppe *et al.*, 1992).

River orientation

In foreland basins, it is useful to define two major river patterns, each of which can be subdivided. In a regional context, longitudinal rivers flow parallel to the main trend of the orogen and the fold-and-thrust belt, whereas transverse rivers flow approximately orthogonal to the thrust belt and are usually tributary to the longitudinal rivers (Fig. 1). Transverse rivers can originate in the hinterland and have a large catchment within the uplifted and eroding part of the orogen, or they may have catchments almost exclusively within the foreland itself. As used herein, transverse rivers flow approximately perpendicular to and away from the orogenic hinterland. In most cases, at any given point in the foreland, transverse rivers with extensive hinterland catchments will have considerably greater discharges and enhanced stream power in comparison to those rivers flowing on similar gradients, but having local catchments within the foreland.

In the context of individual folds or thrusts, river orientation can be defined as either orthogonal to the structural trend or parallel to it. In the latter situation, locally strike-parallel rivers do not traverse a structure, but instead may occupy a position either in the piggyback basin (Ori & Friend, 1984) on the backlimb of the structure or in the forelimb or footwall basin in front of the structure. Rivers with catchments on the fold itself are typically orientated at a high angle to the fold axis and may flow either down the backlimb into the piggyback basin or down the forelimb into the foreland (Fig. 1).

Antecedent rivers

Antecedent rivers have established a course prior to the growth of a structure, such as a fold, and subsequently maintain a course across a developing zone of active differential uplift, rather than being deflected around it. Because most fold axes are orientated at high angles to the overall shortening vector and are parallel to the orogenic axis, antecedent rivers which traverse such folds are often transverse rivers. In order to sustain a course across the zone of maximum bedrock uplift within a given structure, a river has to maintain a forelandward-dipping gradient throughout the deformation. In response to a locally rising base level across a fold crest, therefore, a river may aggrade to maintain its previous gradient upstream of the fold and/or it may erode the fold crest. If it cannot aggrade sufficiently rapidly upstream of the fold crest, the river's slope will decrease in response to the folding.

At least two ratios influence a river's ability to maintain its course across a growing structure. Here, we use a growing fold as an example, but a thrusted hangingwall

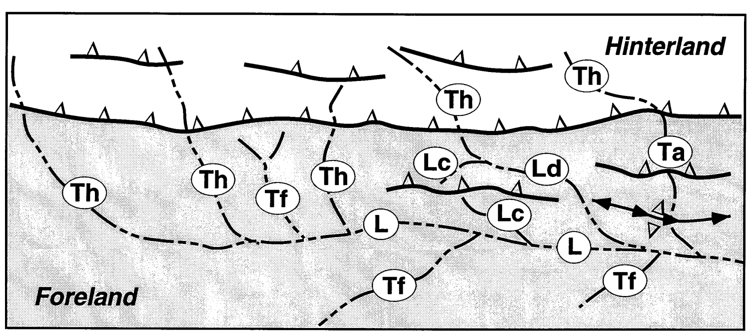

Fig. 1. Conceptual depiction of river orientations in a peripheral foreland basin. Thrusts delineate the uplifting and eroding hinterland and disrupt the proximal part of the foreland. Transverse rivers with hinterland catchments (Th) and with catchments exclusively within the foreland (Tf) are tributary to the longitudinal river (L) which flows in a medial position in the foreland. Transverse rivers (Th) can be diverted by a thrust such that they flow longitudinally within the piggyback basin above the hangingwall (Ld), or they may maintain their antecedent courses (Ta), undeflected across a thrust. Some thrusts or folds uplift parts of the foreland which subsequently act as local catchments (Lc) for rivers which may flow into piggyback basins or into the foreland.

responds to similar influences. We assume that we are in an actively subsiding and aggrading basin in which a fold begins to grow beneath the active depositional surface. First, the ratio of the rate of aggradation adjacent to the fold to the rate of structural uplift of the fold crest determines whether positive topography develops above the growing structure (Table 1). As long as aggradation keeps pace with or exceeds the rate of structural uplift, a transverse river can maintain an antecedent course across a growing structure. In such cases, no topographic relief may develop, despite the ongoing folding of the subsurface. Although the depositional surface may appear unperturbed, the wedge-shaped geometry of syndeformational sedimentary beds in cross-section will reveal the progressive growth of the fold and can be used to reconstruct sequentially the geometry of deformation (Vergés *et al.,* 1996). In general, beds will thin across the crest of the fold (Fig. 2) and, in the case of buckle or detachment folds, will be rotated in the fold's forelimb (Riba, 1976; Anadon *et al.,* 1986; Burbank & Vergés, 1994). Analysis of the stratigraphy of rocks on either side of the fold crest should reveal palaeocurrent directions indicating flow toward the fold axis on its upstream side and away from it on the downstream side. In addition, reconstructed channel cross-sections and palaeodischarge estimates should indicate that similarly sized rivers were active on both fold limbs. If the rivers on the downstream side appear to be considerably smaller in channel size or discharge than those on the upstream side, the upstream river was probably deflected by the fold and did not cross it (Table 2).

If positive topography develops above the depositional plain because the rate of structural uplift exceeds the rate of aggradation, then a second ratio, that of stream power vs. erosional resistance (Bull, 1991), is added to the competition between aggradation and uplift rates in order to determine whether an antecedent river can maintain its course across the fold. When uplift exceeds aggradation, the river must be able to erode the crest of the fold at a rate equal to the difference between the uplift and aggradation rates in order to sustain a forelandward gradient across the uplifting back limb of the fold. If the potential role of transverse structures is ignored, the resistance to erosion of the uplifting fold crest is primarily a function of its lithological character. In general, during the initial stages of folding in terrestrial

Table 1. Controlling variables for persistence of antecedent streams crossing growing folds.

Variable	Effect
Rate of sediment aggradation	Higher rates of aggradation promote persistence of antecedent stream: less erosion required of hangingwall
Rate of structural uplift	Higher rates of structural uplift require higher rates of erosion and/or aggradation to promote persistence of antecedent stream
Resistance to erosion of rocks in hangingwall	Higher resistance requires greater stream power for persistence of antecedent stream. Thick alluvial strata, poor cementation, readily eroded bedrock promote persistence
Discharge and stream power of antecedent stream	Higher discharge and higher stream power promote persistence of antecedent stream
Width of structure	With fixed base level, widening structures cause lowered stream slope and stream power, promoting defeat of antecedent streams
Sediment load	Increased load decreases proportion of stream power available to erode bed; mantling of bed with sediment precludes erosion of bed
Transverse structures	Provide zones of less resistant rocks that cut across structures, exploited by antecedent streams

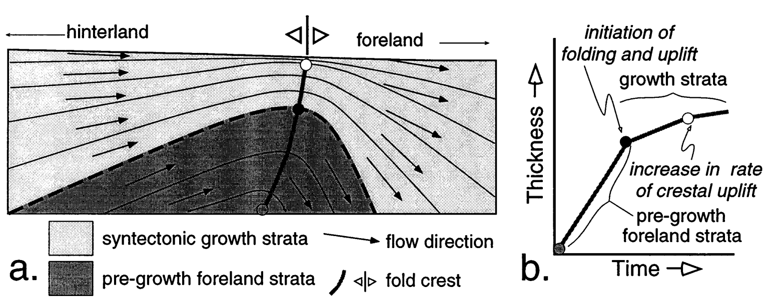

Fig. 2. (a) Cross-section of fold affecting previously deposited foreland strata which display a constant thickness across the fold crest. Note that, because aggradation is more rapid than crestal uplift, the fold never has a topographic expression. For this antecedent river, palaeocurrents indicate flow across the anticline throughout its growth. Bedding geometries across the fold crest show pinching toward fold crest and progressive rotation of beds on both limbs. (b) Theoretical sediment-accumulation rates recorded at the crest of the fold depicted in (a). If bedding contacts are assumed to be equally spaced in time, the initiation of folding and uplift is marked by slowing rates of foreland aggradation. Accelerating crestal uplift causes additional reduction of sediment accumulation across the fold crest, but may have little or no direct impact on the accumulation rates above the fold's forelimb and backlimb.

Table 2. Identification of antecedent rivers in the geological record.

Feature	Significance
Palaeovalley developed across fold crest	River traversed fold crest and incised it when fold was elevated above local base level
Projection of contacts between syntectonic strata over the preserved fold crest	Syntectonic strata overlapped, rather than onlapped flanks of fold
Bevelling of fold crest	River traversing fold eroded uplifting crest: sufficient stream power and time to erode laterally
Transverse palaeocurrents on both flanks of fold	River not deflected by fold crest, flowed across it
Similar sized palaeochannel and palaeodischarge on both fold limbs	Same transverse river identifiable on both limbs. River on distal limb is not locally sourced
Hinterland provenance on both limbs in youngest strata	Same source terrain identifiable on both limbs. River on distal limb is not locally sourced

foreland basins, previously deposited alluvial strata experience relative uplift and constitute the exposed fold crest. These rocks are often weakly lithified and readily eroded, such that even small rivers can sustain erosion rates of >1 mm yr^{-1} (Burbank & Beck, 1991). If the total uplift is sufficient to bring more lithified strata to the surface (DeCelles *et al.*, 1991), such as rocks of a carbonate-rich succession underlying the basin, the resistance to erosion will greatly increase and the likelihood of maintaining an antecedent course will decrease. Thus, the thickness of alluvial strata in foreland basins, the character of the pretectonic strata beneath the foreland and the magnitude of uplift of an individual structure will determine changes in erosional resistance during folding.

Stream power is proportional to the change of kinetic energy along a river's course. This change can be represented as the product of discharge with the local river slope. Because the upstream catchment area is generally proportional to discharge in a given region (Dietrich *et al.*, 1992; Montgomery & Dietrich, 1994), catchment size is often substituted as a proxy for discharge. Thus, antecedent rivers with large hinterland catchments generally have higher stream power and are considerably more likely to maintain their courses across folds than will rivers having similar local slopes, but whose catchments lie primarily within the foreland. Because stream power is also expended in heat and sediment transport, the ability of a river to incise its bed is a function of the proportion of the stream power which is available for erosion. Increasing sediment loads will decrease the work that can be done to erode the river bed. Clearly when unentrained sediment mantles the bedrock beneath a channel, no erosion of the underlying bedrock can occur. During folding, however, fold growth itself tends to decrease the river gradient across the upstream limb, and if a river was in a previous equilibrium state, i.e. at the threshold of critical power (Bull, 1991), this will promote upstream deposition. Assuming no increases in the flux of sediments from hinterland sources, deposition on the upstream fold limb will increase the proportion of the stream power available for erosion as the river traverses the actual fold crest. Moreover, because folding increases the slope of the forelimb, the total stream power will also increase.

Because deformation at time-scales of hundreds of years often is seismically induced, rather than occurring via slow, continuous deformation, local base levels may be abruptly raised during an earthquake due to surface faulting or to uplift during co-seismic folding. Whereas large antecedent rivers with flow depths considerably greater than the magnitude of vertical seismic offset will more readily smooth and eliminate seismically induced perturbations along their beds, smaller rivers may be temporarily dammed by offsets. In such cases, they can leave distinctive lacustrine deposits associated with individual seismic events (Meghraoui *et al.*, 1988). When resistant bedrock in the hangingwall is raised by faulting above local base level, it may create a long-lived perturbation in the bed. Groundwater tables can rise upstream of such fault barriers and saturated or poorly drained soils may become increasingly common (Talling *et al.*, 1995).

Modern antecedent rivers often cross folds with positive topographic relief in water gaps. In the stratigraphic record, antecedent rivers can be identified on the basis of palaeovalleys that traverse the axis of a fold and that can be shown to have formed synchronously with folding (Fig. 3). In these cases, fluvial deposits located downstream or upstream with respect to the fold axis are likely to be folded, as well. The presence of antecedent rivers in the past can be inferred from: persistent transverse (hinterland-to-foreland) palaeocurrents on both sides of the structure; a hinterland provenance represented by sediments on both flanks of the fold; erosionally bevelled crests of folds; and channel bodies in the fold's forelimb (foreland-side) whose sizes are comparable to channel bodies found on the hinterlandward side of the fold, and whose sizes exceed those likely to occur within catchments developed exclusively on the forelimb (Fig. 3; Table 2).

Interference among multiple structures

During development of a fold-and-thrust belt, folds grow laterally and vertically due to propagation of detachments and thrusts and to accumulated shortening (Scholz *et al.*, 1993; Dawers & Anders, 1995). Moreover, several folds may grow concurrently both along and across strike. This can result in folds whose axes are aligned, en echelon folds with offset axes and serial folds representing a fold train extending toward the foreland from the hinterland.

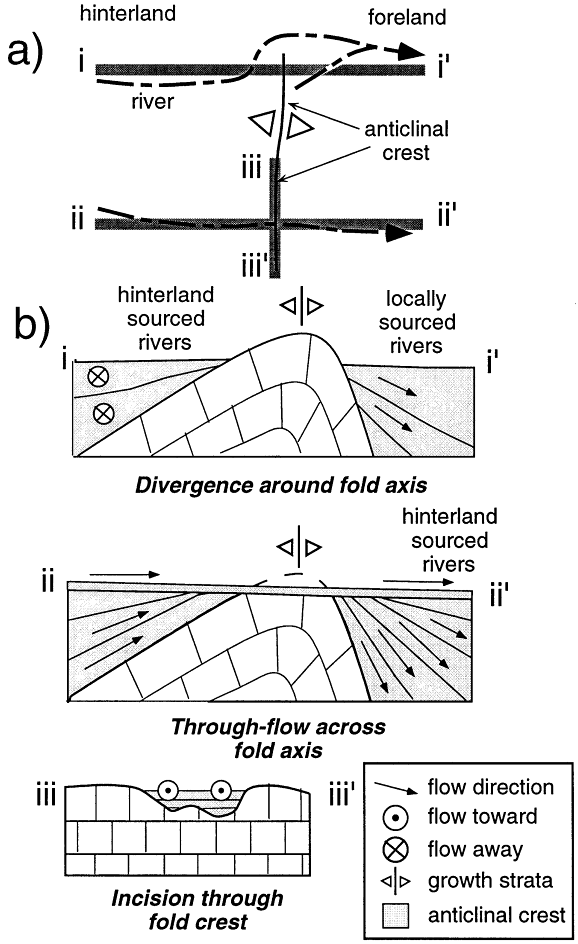

Fig. 3. Stratigraphic characteristics related to rivers that are either antecedent to or are deflected by a growing structure. (a) Map view of deflected river with local river developed on fold's forelimb (top) and undeflected river crossing anticline (bottom). (b) Schematic stratigraphic cross-sections. Cross-section i–i': deflected river. On backlimb, a large, hinterland-sourced river is deflected parallel to the fold crest, whereas a smaller river flows off the forelimb. Cross-section ii–ii': antecedent river in which flow continuously crosses fold crest. Rate of structural uplift is greater than the rate of aggradation: therefore, the river must bevel off the top of the rising fold. Cross-section iii–iii': antecedent river flowing in valley incised across the crestal part of the fold (viewed toward the hinterland).

Although it is often assumed that structures are active sequentially along any given transverse section through a fold-and-thrust belt, the distribution of modern seismicity (Seeber *et al.*, 1981), Holocene faulting (Dolan *et al.*, 1995) and stratigraphic evidence (Burbank *et al.*, 1992) indicate that distributed deformation persists on time-scales ranging from hundreds to hundreds of thousands of years.

The response of antecedent fluvial systems to an array of growing folds (Fig. 4) is an extension of the response of an antecedent river to a single fold. If aggradation is more rapid than uplift of any fold or if stream power is sufficiently high, river courses will be undeflected. Even when folds are topographically expressed, water gaps developed by rivers with large discharges and stream power can serve to fix the position of antecedent rivers through successive folds (Talling *et al.*, 1995). In contrast, if transverse rivers are 'defeated' or deflected by growing folds, they will tend to be diverted around structural culminations and through structural low points or saddles between plunging folds (Fig. 4).

Palaeotopography and drainage localization

Although a planar, subhorizontal geometry for the pretectonic strata is commonly assumed at the time of initiation of a new phase of deformation, these strata have often been affected by previous episodes of tectonism. If earlier deformational events involved sufficient uplift to elevate resistant strata above the local base level, then positive topographic relief could be present at the time of any subsequent deformation. Such relief is modified by erosional processes, which tend to bevel topography that stands above local base level, and by subsequent deposition, which can onlap or cover pre-existing topography. The topographic relief that exists at the initiation of a deformational interval is therefore a function of the magnitude of previous intervals of tectonic uplift, changes in local base level since that uplift, lithological resistance to erosion, climatic conditions and the time since deformation (Beaumont *et al.*, 1992). In semi-arid and arid climates, for instance, carbonate strata are highly resistant and often define long-lasting local relief, whereas carbonates may be more readily dissolved in humid climatic conditions. Any relief that exists at the initiation of a new depositional or deformational cycle will exert strong controls on the localization of fluvial channels which will follow the locus of low points within that landscape.

Palaeotopography, defined as inherited topographic features created prior to the interval of interest, can be recognized at a variety of scales in the stratigraphic record. At the large scale, the thickness of syntectonic alluvial strata that fill a palaeovalley can define a lower limit on the magnitude of pretectonic topographic relief (Burbank & Vergés, 1994). At mesoscales, passive and high-angle onlap of valley walls and buttress unconformities define former valley margins (Fig. 5), whereas karstified or deeply weathered surfaces can define high-standing surfaces into which palaeovalleys were incised.

A strong contrast in topographic relief is typically found between the orogenic hinterland and the low-standing foreland. Valleys incised through hinterland topography may be orientated at high angles to subsequent shortening directions, especially in areas where weakly resistant zones within strike-parallel structures have been erosionally exploited. When such a hinterland river debouches into the foreland, often the fluvial regime switches from one of erosion and transport to one of deposition in the proximal foreland. If the local base level in the foreland is rising and sediments accumulate sufficiently rapidly, valleys within the hinterland can be

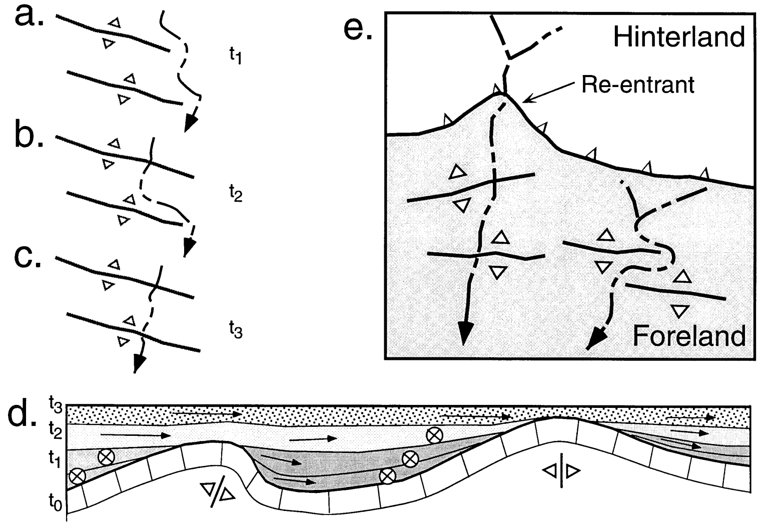

Fig. 4. Conceptual orientations of rivers with respect to successive fold crests that develop synchronously in a foreland. (a) Both anticlines deflect the river. (b) Only the outer anticline deflects the river. (c) River traverses both anticlines and could be considered antecedent. (d) Schematic cross-section of serial anticlines that developed synchronously. Each stage in deposition (t_1, t_2, t_3) depicts the palaeocurrent orientations and large-scale bedding geometries that would be expected given the river-to-fold relationships depicted in (a)–(c) (with corresponding labels of t_1–t_3). Cross-sectional geometries are controlled by the relative rates of sediment accumulation to crestal uplift. (e) Theoretical interactions of growing folds with rivers with large hinterland catchments vs. catchments localized in the foreland. Across a comparable gradient, greater discharge of larger river yields a higher stream power and enables it to traverse, rather than be deflected by, the growing anticlines. Note that the hinterland rivers debouche into the foreland through a structural re-entrant.

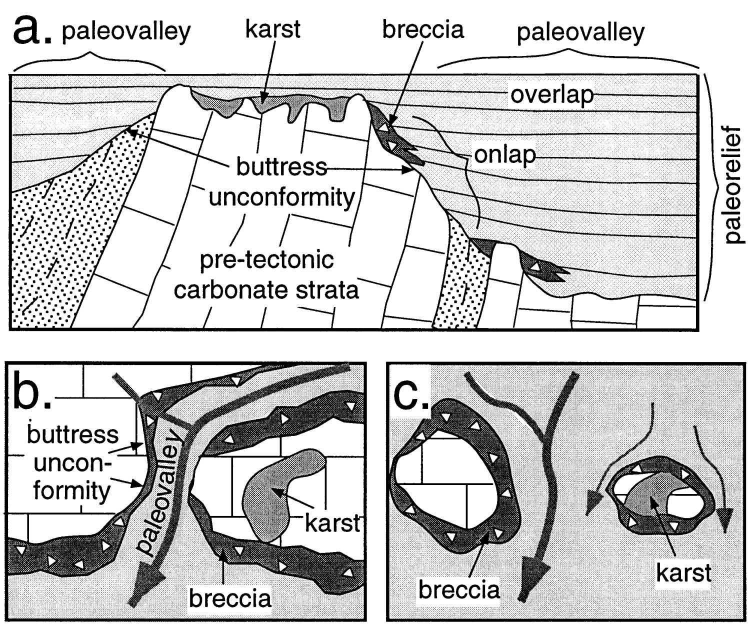

Fig. 5. Examples of stratigraphic characteristics that define palaeotopography and palaeorelief in the stratigraphic record. (a) Resistant carbonate strata create an elevated region in the palaeolandscape. A karst surface develops on the carbonates, whereas less resistant strata are recessively eroded. Young alluvial strata aggrade along a buttress unconformity and interfinger with carbonate breccias and talus shed from the highland. Strata filling the palaeovalleys passively onlap and later overlap the topography; they are not significantly deformed. (b) Schematic map view of palaeovalley incised through resistant carbonate rocks. As younger sediments begin to aggrade, deposition is focused along the palaeovalley. Strata onlap the valley walls (buttress unconformity) and interfinger with breccias. (c) Continuing deposition immerses previous topography and only a few isolated, but elevated regions influence the course of rivers in the foreland.

infilled with alluvial strata (Mellere, 1993). When topography is being immersed beneath accumulating syntectonic sediments, the remaining emergent topography will define the margins of alluvial plains and valleys (Fig. 5) and can be an important local sediment source. In the stratigraphic record, breccias, talus and mass movement deposits are often spatially localized near palaeovalley walls.

The position of drainages can also be influenced by structures that develop synchronously with deposition and erosion. At the leading edge of the emergent hinterland, structural re-entrants can focus hinterland drainage and control their entry points into foreland basins. Despite a conspicuous association of rivers and structural re-entrants (Fig. 4e) along the margins of several foreland basins (Eisbacher *et al.,* 1974; Burbank, 1992), it is often unclear whether the river became localized in the re-entrant as the structure developed or whether interactions between an eroding river and a pre-existing re-entrant (Oberlander, 1985) led to drainage localization. Both within the foreland and within the leading edge of the hinterland, lateral ramps often provide preferred pathways along which rivers exit from piggyback basins in fold-and-thrust belts (Burbank & Raynolds, 1988; Lawton *et al.,* 1994). Erosionally susceptible zones caused by wrench or tear faults within growing folds can also be exploited by antecedent rivers that traverse such structures (Medwedeff, 1992).

Fold-and-fault evolution

Syntectonic strata can faithfully record fold growth and fault motion when deposited in direct association with deforming fold limbs or active fault planes. Most presently exposed folds that developed during a pre-Late Cenozoic deformation, however, are spatially separated from any preserved syntectonic strata due to erosion since the time of folding. Such folds are often interpreted in the context of popular fault-bend or fault-propagation fold models (Medwedeff, 1989; Suppe, 1983), and a kinematic history of fold growth is assumed based on the preserved final geometry and model predictions. In contrast, extensive preservation of syntectonic strata along the fold limbs (herein termed 'growth strata') can permit a step-by-step reconstruction of the shape and growth of a fold (Suppe *et al.*, 1992; Vergés *et al.,* 1996) and can yield an unambiguous record of fold growth.

When growth strata are deposited across a growing fold, they often record limb dip angles and limb length through time. Because the upper surfaces of the growth strata are usually subhorizontal at the time of deposition, post-depositional rotations of such surfaces are easily defined (Riba, 1976). Often such rotations are also associated with growth strata that are tabular in more distal locations, but which either taper or remain tabular as they are incorporated into the fold's forelimb (Vergés & Burbank, 1992; Burbank & Vergés, 1994; Hardy & Poblet, 1994). If tapered, the angle of taper can also be used to define the magnitude of differential uplift and forelimb rotation (Vergés & Burbank, 1992) during deposition (Fig. 6). If untapered, but incorporated in the fold forelimb, such strata provide evidence for lateral growth of the fold and migration of axial surfaces (Suppe *et al.*, 1992). Similar taper and bedding geometries can be used to define rotation of the backlimb, as well. When growth strata are well dated, 'unfolding' of these strata reveals changes in rates of uplift, shortening, forelimb rotation and aggradation (Fig. 6) that can be used to reconstruct the detailed kinematic evolution of a fold (Vergés *et al.,* 1996). Any changes in the forelimb dip can directly affect the stream power of antecedent rivers crossing the fold, whereas uplift of the fold crest affects both gradients and accommodation space upstream of the fold. Thus, a reconstruction of the history of fold growth can define key parameters that control the responses of associated river systems to the folding.

Although thrust faults which actually cut the depositional surface were once considered uncommon, there are numerous modern examples of thrusts which have propagated to and emerge at the surface (Rockwell *et al.,* 1984; Meghraoui *et al.,* 1988). Identification of similar thrusts in the geological past rests largely on interpretation of syntectonic strata. A narrow zone of brecciation is commonly associated both with thrusts that cut older, previously deposited strata and thrusts that extended to the active depositional surface. Rapid facies changes away from a fault, however, and the presence of syntectonic depositional breccias or talus derived from the hangingwall indicate faults that breached the surface (Fig. 7). Syntectonic folding of strata and differential strata thicknesses across a fault may indicate thrusts in the very shallow subsurface.

MODERN EXAMPLES OF GROWING FOLDS AND COEVAL DEPOSITION

When actively growing folds can be identified, it is possible to determine specific interactions of fluvial systems with the deforming structures. Tributary catchments, deflected and antecedent rivers, and the geomorphological products of fluvial deposition and fluvial and hillslope erosion can be analysed. When sufficient data are available, stream power, uplift rates and incision rates can also be calculated. We examine two examples of active folding: Wheeler Ridge in California and the northern Brooks Range in Alaska. Previous structural and chronological studies related to Wheeler Ridge provide a context within which the fluvial systems and geomorphology can be analysed. Although fewer data on the structural and stratigraphic characteristics of the Alaskan folds are known, regional remote-sensing data obtained from satellite images permit clear interactions to be discerned among the modern rivers and active folds.

Wheeler ridge

Located at the interface between the northern flank of the Transverse Ranges (San Emigdio Mountains) and the depositional plain of the southern San Joaquin valley of California, Wheeler Ridge (Fig. 8) represents the outermost major fold in a predominantly north-vergent, fold-and-thrust belt that extends southward across the Transverse Ranges (Namson & Davis, 1988; Medwedeff, 1992). Because it contains a productive oil field, the subsurface structure of Wheeler Ridge has been well studied. Wheeler Ridge is an east–west-trending, east-

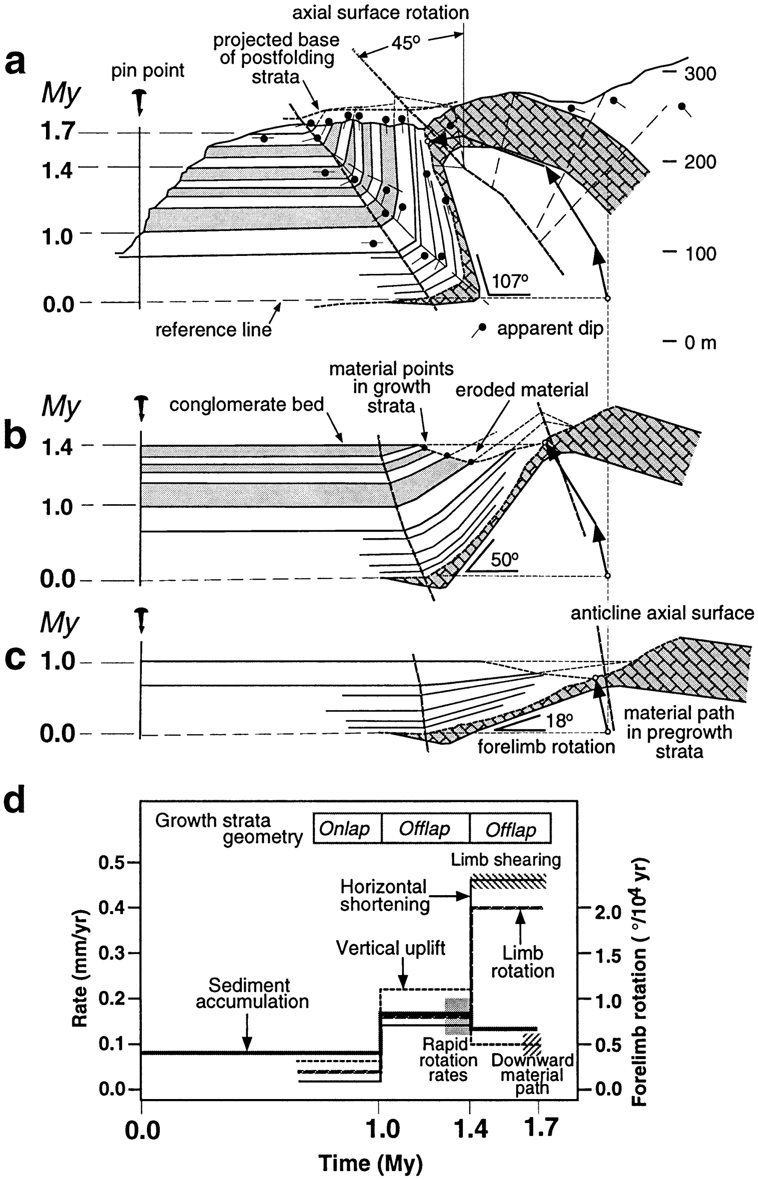

Fig. 6. Reconstruction of the kinematics of fold growth. Based on a process of 'unfolding', the upper surface of each syntectonic stratal unit is restored to horizontal, and underlying units are unfolded or back-rotated by an amount equivalent to the dip removed from the topmost stratum. Stratal areas are preserved during unfolding. Motion of material points, axial surfaces and fold hinges can be reconstructed in each step. (a) Deformed state cross-section at end of folding (1.7 Myr after start) depicting observed bedding geometries in a growth syncline and in the adjacent anticline. Note strata of uniform thickness at the pin line and tapering of beds in the forelimb of the fold. Forelimb is overturned by 17°. (b) Restoration at 1.4 Myr after removal of 67° of forelimb dip. Note material points in growth strata are uplifted with respect to the crest of the anticline in the next youngest step (to 1.7 Myr). This causes pronounced offlap. (c) Restoration at 1.0 Myr after removal of 89° of forelimb dip. Note that the initial path of a material point in the anticlinal crest is upward, and the anticlinal hinge is almost vertical. In younger steps, the anticlinal hinge rolls forward by 45°, and the material point in pregrowth strata moves upward, forward and finally downward. (d) Calculated rates of crestal uplift, shortening, forelimb rotation and aggradation based on unfolding. Modified after Vergés *et al.* (1996).

plunging anticline whose eastern nose is still buried below the modern depositional plain (Figs 8 and 9). It is interpreted to have developed above a wedge thrust (Medwedeff, 1992) that merges into a southward-dipping detachment. The Pleito Thrust emerges a few kilometres closer to the hinterland and is linked to the same detachment surface (Figs 8 and 9). Trending obliquely to the axis of Wheeler Ridge, the Pleito Thrust juxtaposes crystalline hinterland rocks against Neogene alluvial and fluvial deposits. The folded hangingwall at Wheeler Ridge is cut by transverse faults (Medwedeff, 1992) orientated approximately perpendicular to the fold axis and defined by subsurface data, linear trends through the fold and a conspicuous surface offset near the eastern terminus of the surficial expression of the fold (Figs 8 and 9).

Previous studies have shown that growth of the eastern half of the fold (that part described here) initiated at $\approx$90–120 ka (Keller *et al.*, 1989; Zepeda *et al.*, 1990). The emergent nose of the fold has propagated eastward at a mean rate of $\approx$25 m kyr^{-1} (Medwedeff, 1992). Within the uncertainties of the ages assigned to uplifted surfaces, the mean rate of crestal uplift of the emergent fold has been $\approx$3–3.5 m kyr^{-1}, whereas sediment-accumulation rates in the undisturbed plains beyond the folded domain have averaged $\approx$2 m kyr^{-1} during the past 100 kyr (Medwedeff, 1992).

The modern-day geomorphology provides a clear 'snapshot' of the effects of the time-integrated interactions between the growing anticline and the extensive alluvial-fan complex emerging from the San Emigdio Mountains (Figs 8 and 9). Despite this view of the present landscape, it is difficult to quantify unambiguously how the interactions over long time spans of fluvial and hillslope processes with the rates and patterns of

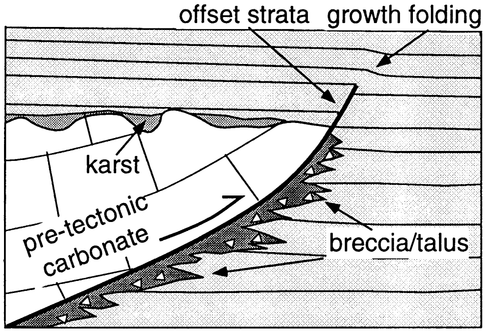

Fig. 7. Conceptual model of stratigraphic record of a thrust that uplifted its hangingwall at the same rate that syntectonic strata aggraded in front of it. For most of its history of motion, the thrust overruns its own talus/breccia which grade abruptly into adjacent flat-lying beds. As thrusting wanes, strata overtop the pretectonic carbonate strata. These beds are initially offset by the thrust, and younger ones are folded above the projection of the thrust.

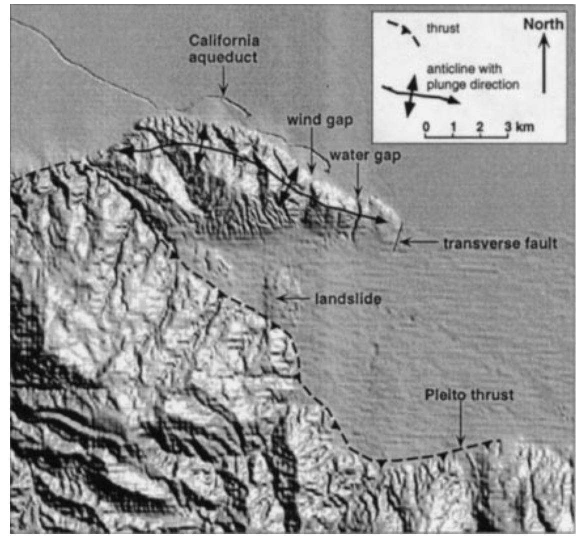

Fig. 9. Shaded relief map of US Geological Survey 30-m digital elevation data from the southern San Joaquin Basin, Wheeler Ridge and the San Emigdio Mountains. Illumination direction is from the NE at 45°. Note the clear eastward plunge of the fold, the variation in the dissection along its length, the contrast in slope and dissection between its forelimb and backlimb, and the presence of water and wind gaps.

structural uplift have resulted in the observable drainage patterns and geomorphology. Some insights on these interactions, however, can be gained from analysing the modern topography.

The emergence of the fold above the depositional plain has strongly perturbed the fluvial patterns south of Wheeler Ridge. An aggrading piggyback basin lies between the Pleito Thrust and Wheeler Ridge, and a broad, gently north-sloping alluvial plain surrounds the east and north sides of the fold (Figs 8 and 9). Because the Pleito Thrust trends obliquely to the axis of Wheeler Ridge and because it rides up on to the western end of the fold, the piggyback basin between the Pleito Thrust and the fold is topographically closed to the west. Consequently, rivers that fail to cross the anticline must flow toward the east (Figs 8 and 9), where they join others and are either focused into a water gap or are diverted around the plunging nose of the anticline. On the distal, northern flank of Wheeler Ridge, short-radius (generally <1 km), locally sourced alluvial fans are being actively deformed in their proximal parts by the growing fold which is incorporating them into its forelimb (Fig. 8). The topography of the large alluvial fans which sweep around the north-east and north-west sides of Wheeler Ridge suggests that they also have been deflected around the growing anticline. Adjacent to the north side of the anticline, which is downstream with respect to the regional drainage system, these large fans converge (Fig. 8) toward a zone of reduced accumulation: a 'depositional shadow zone'. Antecedent rivers have exploited

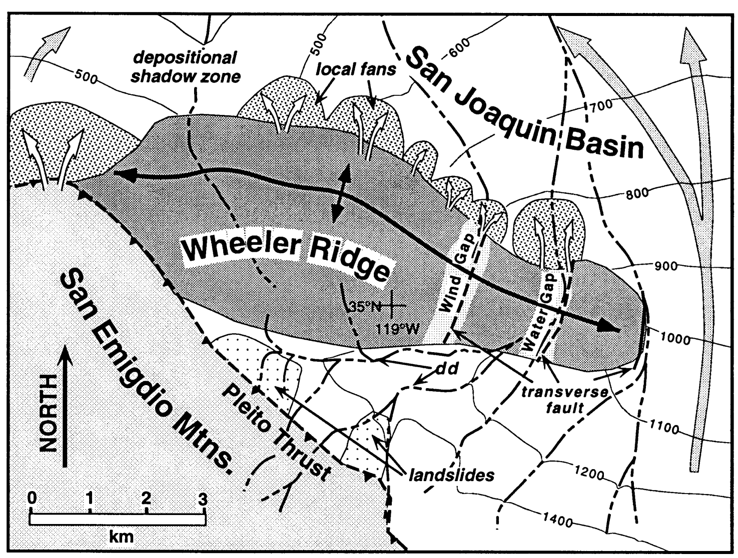

Fig. 8. Geomorphological map of Wheeler Ridge, southern San Joaquin Basin, California. Major structural elements, and the locations of wind gaps, water gaps, transverse faults, locally derived fans and landslides are shown. A piggyback basin lies between Wheeler Ridge and the San Emigdio Mountains. Several drainages within the piggyback basin, as well as the regional drainage pattern, have been deflected by the rise of the anticline. dd: deflected drainage.

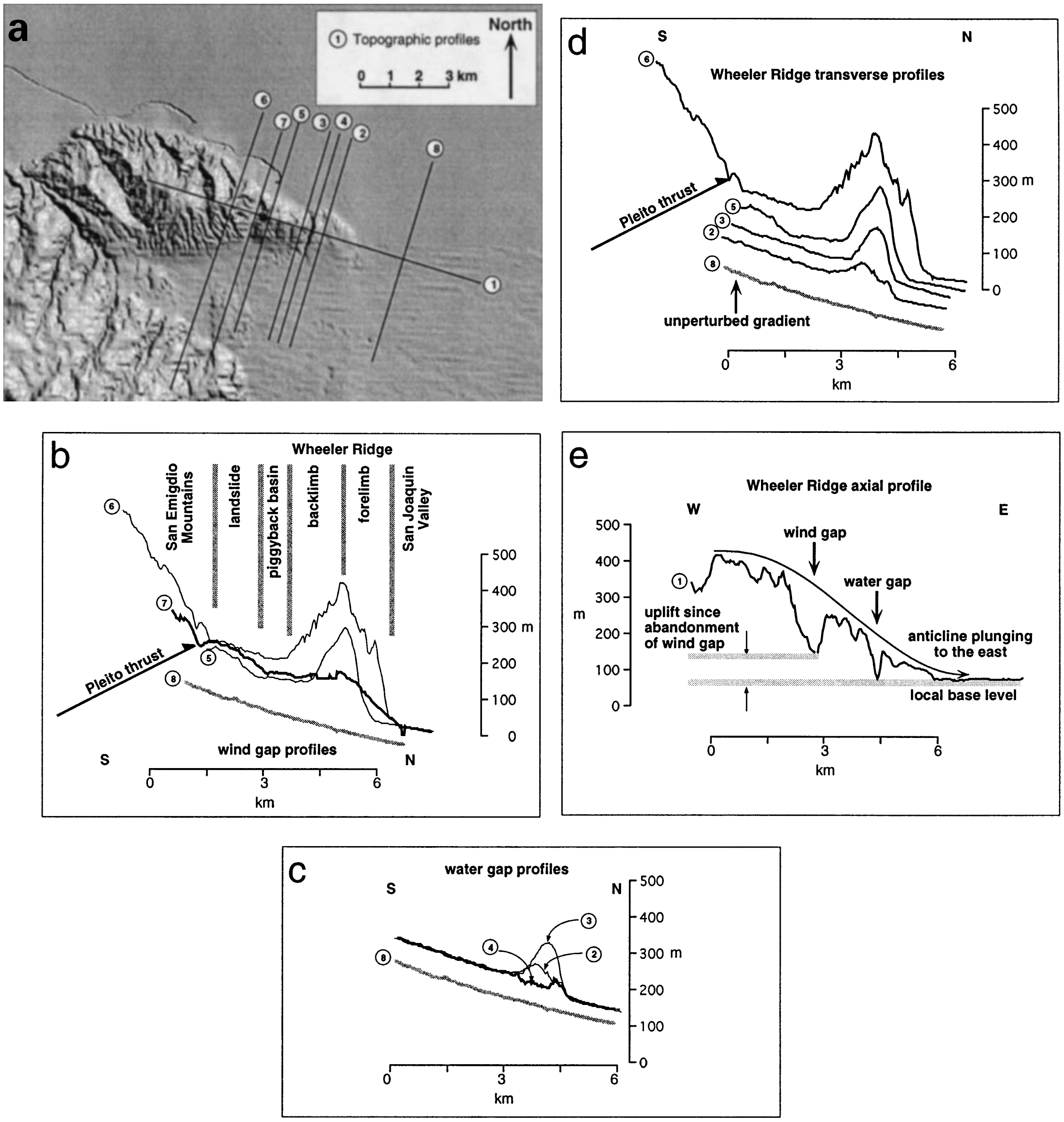

Fig. 10. (a) Shaded digital topography of the Wheeler Ridge region showing locations of topographic profiles. (b) Topographic profile from the San Emigdio Mountains, across the Pleito thrust, and through the wind gap (profiles 5–7). For reference, the gradient of the unperturbed alluvial fan to the east of Wheeler Ridge (profile 8, Fig. 11a) is shown. In comparison to the unperturbed profile, the wind gap profile is steeper on the forelimb of the fold and more gentle both on the backlimb and within the piggyback basin. The frontal gradient through the wind gap is less steep, however, than the fold forelimb because an alluvial fan has been built on the downstream side of the wind gap. Topographic steps in the profile represent topographic fronts related to the toe of a landslide and the Pleito thrust. Adjacent profiles cross the Wheeler Ridge anticline on the west (profile 6) and east (profile 5) sides of the wind gap. Comparison between the profile through the wind gap with the unperturbed profile indicates the amount of uplift since abandonment. Comparison of the wind gap profiles with adjacent profiles indicates the amount of incision of the river in the wind gap prior to its abandonment. Note the flattened segment of the topography within the piggyback basin. (c) Topographic profiles through water gap (profile 4) and through adjacent fold crests: east (2) and west (3). Note the near parallelism of the gradient through the water gap with the unperturbed profile. Only a minor amount of filling of the piggyback basin is evident. Profiles adjacent to the water gap indicate at least 100 m of incision since the antecedent stream began to erode the rising anticline. (d) Successive profiles across the Wheeler Ridge anticline. The amplitude and width of the fold increases from east to west. The shape of the fold is quite constant and displays a steeper forelimb than backlimb. (e) Topographic profile along axis of fold (profile 1) showing plunge to east, elevated floor of wind gap, and the equivalent altitudes of the water gap and the eastern termination of the fold. Height of the base of the wind gap above the local base level defines the amount of uplift since abandonment. Each of the major topographic breaks is associated with a transverse fault.

several of the transverse structures (Medwedeff, 1992) which form weaknesses across the fold. The past and present courses of two such rivers are represented by a wind gap and a water gap within the uplifted part of the fold and by a stream which flows adjacent to the fold's surficial termination. Along the former river course through the wind gap, the highest point is situated ≈230 m below the crest of the fold and ≈70–80 m above the reconstructed gradient of the river just prior to abandonment of its course across the fold (Fig. 10b). Thus, erosion by this antecedent river managed to keep pace with uplift during the first 75% of its growth above local base level.

Why was the river course in the wind gap abandoned, whereas the river within the water gap at present is capable of maintaining its course? Although the answer clearly resides in the balance between river incision and crestal uplift, it is not possible to isolate definitively a single variable that accounts for the defeat of the stream that flowed through the wind gap. Within the uncertainty of the published ages (Keller *et al.*, 1989; Zepeda *et al.*, 1990) of surfaces along the axis of the fold, there is no clear acceleration in the rate of fold uplift over time nor does the mean uplift rate change significantly along the exposed fold. Thus, it appears that the transverse river was not required to incise more rapidly through time. It is clear that, as the fold grew, it broadened (Fig. 10d), such that the river had to incise through a widening region of uplift. It is likely, moreover, that increasingly lithified strata were being exposed at the erosional surface due to incision through the core of the growing fold. If discharge was held constant through time, then the river in the present wind gap may have been defeated because increases in slope and resultant stream power were unable to counterbalance increasing bedrock resistance (Bull, 1991).

Alternatively, river avulsion and stream capture can be explained as a natural result of continuing aggradation behind the growing anticline, without the need for a variation in either bedrock resistance or structural uplift rate. In this scenario, the river flowing through the future wind gap ultimately avulses toward the east and is captured by an existing river that is flowing through the water gap. Prior to this, when the anticline initially begins to emerge above the alluvial surface, the river gradient steepens across the forelimb of the uplifted zone (Figs 11 and 12). This enhances stream power and erosion on the forelimb, but also causes aggradation in the piggyback basin due to the lowered gradient there which results from folding (Fig. 11b,d). A stream-profile knickpoint is generated at the junction of the fold forelimb with the depositional plain. Unless this knickpoint manages to migrate upstream through the entire width of the uplifted area and across the piggyback basin prior to the next deformation episode, both a steepened gradient across the fold itself and at least some of the newly aggraded strata within the piggyback basin will persist into the next episode of folding. Thus, as the fold

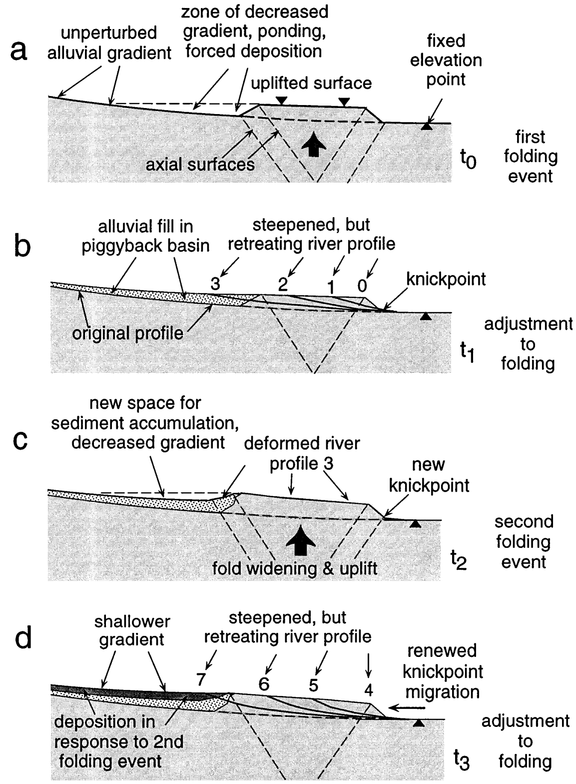

Fig. 11. Schematic cross-sections of aggradation in piggyback basin and river-profile changes during fold growth. (a) Initial profile (dashed) deformed by uplift. Equal amounts of bedrock uplift occur across the crest of the anticline, but the surface of the anticline slopes toward the basin, due to the vertical displacement of the pre-existing fluvial gradient. Note the gentle gradient and new accommodation space upstream of the fold. (b) Uplift causes steepening of river gradient in forelimb and aggradation in piggyback basin, where the gradient flattens. Knickpoint migrates upstream and flattens perturbed river profile through time (positions 0–3). (c) Next increment of uplift (same vertical magnitude) causes widening of the anticline, folds pre-existing fluvial surface (3), creates new knickpoint and raises base level within the piggyback basin. (d) More aggradation occurs in the piggyback basin as knickpoint migrates upstream and profiles (positions 4–7) become smoother and gentler through time.

continues to widen (Fig. 11c,d), continued deposition is forced by the folding and will raise the height of the surface of the piggyback basin upstream of a water gap (Fig. 12). Because the fold is propagating toward the east, enhanced deposition occurs in the western part of the piggyback basin and creates an eastward gradient within the basin. When combined with the fact that the Pleito Thrust overrides Wheeler Ridge and closes the piggyback basin to the west (Figs 8 and 9), avulsion out of this elevated and aggraded part of the basin would divert the river to the east.

The persistence of the present river in the water gap may be accounted for in several ways. The fold is of lower amplitude (Fig. 10c), such that less resistant strata

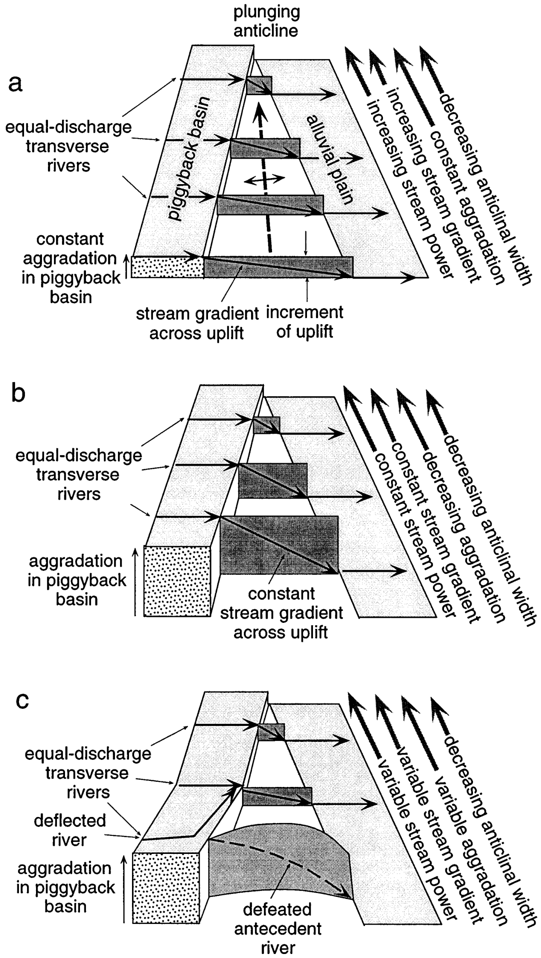

Fig. 12. Schematic models of aggradation in piggyback basins and variable river gradients across growing, plunging anticline. (a) Variation in gradients across a rising structure as a function of fold width. An equal amount of uplift is assumed along the entire structure. Aggradation in the piggyback basin is sufficient to allow transverse rivers to flow directly into the water gaps. The comparative stream gradients among the rivers are a function of the variable width of the uplift. Given equal-discharge transverse rivers, the narrowest part of the structure has the steepest gradient and the highest stream power. (b) If the stream gradient across the uplifted area is the same in each transect, then as the structure widens, the amount of aggradation in the piggyback basin must also increase. The resulting elevation increase in the piggyback basin could promote avulsion and deflection of the transverse river flowing across the widest part of the uplift. (c) If a transverse river is defeated, its previous course across the fold will be warped by continuing uplift and its discharge will augment that of another river. Given the enhanced discharge, the expanded river can display higher or equivalent stream power, despite a lower gradient across the fold, and it can still incise at a pace equivalent to the uplift rate.

are exposed to erosion. Its catchment, and presumably its discharge, is more than six times larger than that of the river which traversed the wind gap. Thus, greater stream power could be maintained, even on a significantly lower slope than that through the water gap when it was occupied by an antecedent river.

Comparison of the topographic profiles through the wind and water gaps is instructive (Fig. 10b,c), especially when compared with the 'unperturbed' profile east of the fold (#8, Fig. 10). In the vicinity of the wind gap, the gradient across the backlimb of the fold and the piggyback basin is much lower than the unperturbed gradient, and up to 100 m of sediments appear to have accumulated within the piggyback basin. By comparing the profiles through and on either side of the wind gap (Fig. 10b), the eastward slope of the surface of the piggyback basin is apparent. These observations are consistent with the models presented above and suggest that aggradation in the piggyback basin may play a key or controlling role in the defeat of formerly antecedent rivers. Topographic profiles through the water gap (Fig. 10c) are nearly parallel with the unperturbed profile, both upstream and downstream of the fold. About 30 m of aggradation has occurred upstream of the fold, however, and the stream gradient is steeper across the fold itself. Whereas these observations are consistent with the models, the absence of a lowered surface gradient within the piggyback basin is not. Instead, it appears that the water and sediment fluxes across the piggyback basin have been sufficient to re-establish the gradient that existed prior to folding.

In the context of conceptual models of responses to folding (Figs 2–5) that would be recorded at Wheeler Ridge in the stratigraphic record, i.e. in the subsurface, we would expect to see no significant change in provenance on either side of the fold, even after defeat of the stream which flowed through the present wind gap, because the gravels being uplifted and eroded in the fold are similar to those being carried out of the San Emigdio Mountains today. When comparing strata that were deposited on the distal, north side of the fold prior to and following the defeat of the stream through the wind gap, however, we would see significant increases in the mean depositional slope and reductions in the size of channels, their lateral extent, and calculated palaeodischarges. Following defeat of the stream that flowed through the wind gap, increases in palaeodischarge and slight decreases in depositional slope or grain size might be expected in the vicinity of the water gap. Within the piggyback basin along transects from west to east and from old to young, we would also expect to see palaeodischarge increases and a greater proportion of channels orientated parallel to the anticline as defeat of antecedent streams diverted flow toward to east.

Alaska North Slope and Brooks Range

Another perspective on interactions between rivers and growing structures can be derived from remotely sensed data of surficially expressed folds. Based on satellite images of active fold-and-thrust belts, patterns of deflected, defeated and antecedent streams can be defined with respect to folded structures, and interpretations can be made of the changing balance between stream power, incision rates and uplift rates.

Two surficial anticlinoria developed near the leading edge of the north-eastern Brooks Range fold-and-thrust belt in northern Alaska, the Sadlerochit Mountains and Marsh Creek anticlinoria (Bader & Bird, 1986; Kelley & Foland, 1987; Meigs, 1990; Wallace & Hanks, 1990), have profoundly impacted the fluvial network which lead from the Brooks Range to the Beaufort Sea (Fig. 13). Although the deformation in this region probably initiated in the early Palaeocene (O'Sullivan *et al.,* 1993), late Neogene deformation in the coastal plain and in the Sadlerochit Mountains is indicated by stratigraphic, geomorphological and seismological data (Grantz & May, 1982; Bader & Bird, 1986; Kelley & Foland, 1987; Russell & McMillen, 1987; Combellick, personal communication). Observation of the distribution of rivers and the positions of wind and water gaps with respect to these two anticlinoria implies that the deformation related to both these structures is on-going.

On the north, the Marsh Creek anticline is expressed at the surface by folded upper Cretaceous to Pliocene clastic rocks of the foreland-basin succession (Fig. 13) (Grantz & May, 1982; Bader & Bird, 1986;Kelley & Foland, 1987). Folding is interpreted to be a reflection of intense structural thickening in older rocks at depth (Kelley & Foland, 1987). Three rivers, the Katakturuk River, Marsh Creek and the Sadlerochit River, flow from south to north across the crest of the east-plunging fold (Fig. 13). A difference in discharge between the three rivers is suggested by the size and location of their catchments. Overall, there is a south-to-north decrease in precipitation across the Brooks Range, so that catchments in the south will have higher discharges than similarly sized catchments in the north. Marsh Creek's catchment lies entirely within the Sadlerochit Mountains on the north side of the range, the Katakturuk River drains both the Sadlerochit and Shublik Mountains, and the Sadlerochit River drains portions of each of these ranges, as well as a significant area of the Brooks Range to the south of the study area (Fig. 13) (see also U.S.G.S. Mt Michelson 1 : 250 000 quadrangle). The courses of both the Katakturuk River and Marsh Creek change orientation over short reaches where they encounter the anticline. Marsh Creek flows to the north-east, parallel to the contact between lower and upper Tertiary rocks on the south-east limb of the fold for several kilometres before turning northward across the crest of the fold. In contrast, the Katakturuk River flows across the crest before flowing parallel to the contact between the two Tertiary units on the north-west limb of the fold. The Katakturuk River's greater discharge and inferred greater stream power may explain why it flows across the crest of the fold, whereas Marsh Creek is diverted parallel to it. Given that these streams on opposite sides of the fold are localized along the same lithological contact, differential erodability of dipping beds appears to exert an important primary control. The Sadlerochit River maintains an undeflected path across the coastal plain. Given that the Marsh Creek anticline is seen in the subsurface to the north-east of the Sadlerochit River, it seems likely that the river's stream power has been sufficient to maintain its course in the face of continued uplift of the anticline.

Geomorphology to the south in the Sadlerochit Mountains indicates contrasting long-term histories for the Katakturuk and Sadlerochit Rivers. The Katakturuk River occupies a deeply incised water gap which traverses the narrow, western part of the range (Fig. 13). The Sadlerochit River, in contrast, flows around the eastern nose of the Sadlerochit Mountains anticlinorium. The prominent Sunset Pass wind gap traverses the broader eastern portion of the range (Fig. 13). This map configuration is remarkably similar to that observed at Wheeler Ridge (Fig. 8). Spatial association of a wind gap near the termination of a plunging anticline and diversion of a river around the anticline's nose suggests that the Sadlerochit River once flowed through the Sunset Pass wind gap and was forced to relocate as the anticlinorium continued to rise and the river could no longer keep pace with the rate of uplift. Today, the low point in the wind gap is only 200 m above the alluvial plain to the south, whereas it lies >750 m below the ridge crests on either side of the gap. This suggests that, during the initial 750 m of uplift above local base level, the river successfully incised through the growing structure, and that only recently was the river diverted.

As at Wheeler Ridge, the river's diversion could be attributable to several causes: lowering of the stream gradient across a broadening structure that caused a reduction in stream power, aggradation within the piggyback basin causing avulsion, changes in discharge or sediment load or changes in bedrock resistance. In the Brooks Range, it is also possible that diversion had another cause: Pleistocene glaciers blocking drainages and re-directing rivers along their margins. Remotely sensed data cannot indicate which is the most likely cause, but can help to eliminate some possibilities. The reach of the river where it crosses the range is about twice as long for the Sadlerochit River as for the Katakturuk River. Given approximately the same vertical drop across the structure (200 m), the slope of the Sadlerochit River would be about half of that of the Katakturuk River, and for comparable discharges, stream power would be decreased by this amount in the Sadlerochit River: this could cause abandonment as the zone of uplift widened. The catchment of the Sadlerochit River and its inferred discharge, however, is 6–10 times greater than that of the Katakturuk River. Therefore, despite a lower slope, its stream power should still be 3–5 times greater and should not be the cause of abandonment.

The bedrock is very similar at both the water and wind gaps, so that differential bedrock resistance is unlikely to have caused abandonment of the course through the wind gap. If discharge, river width, uplift

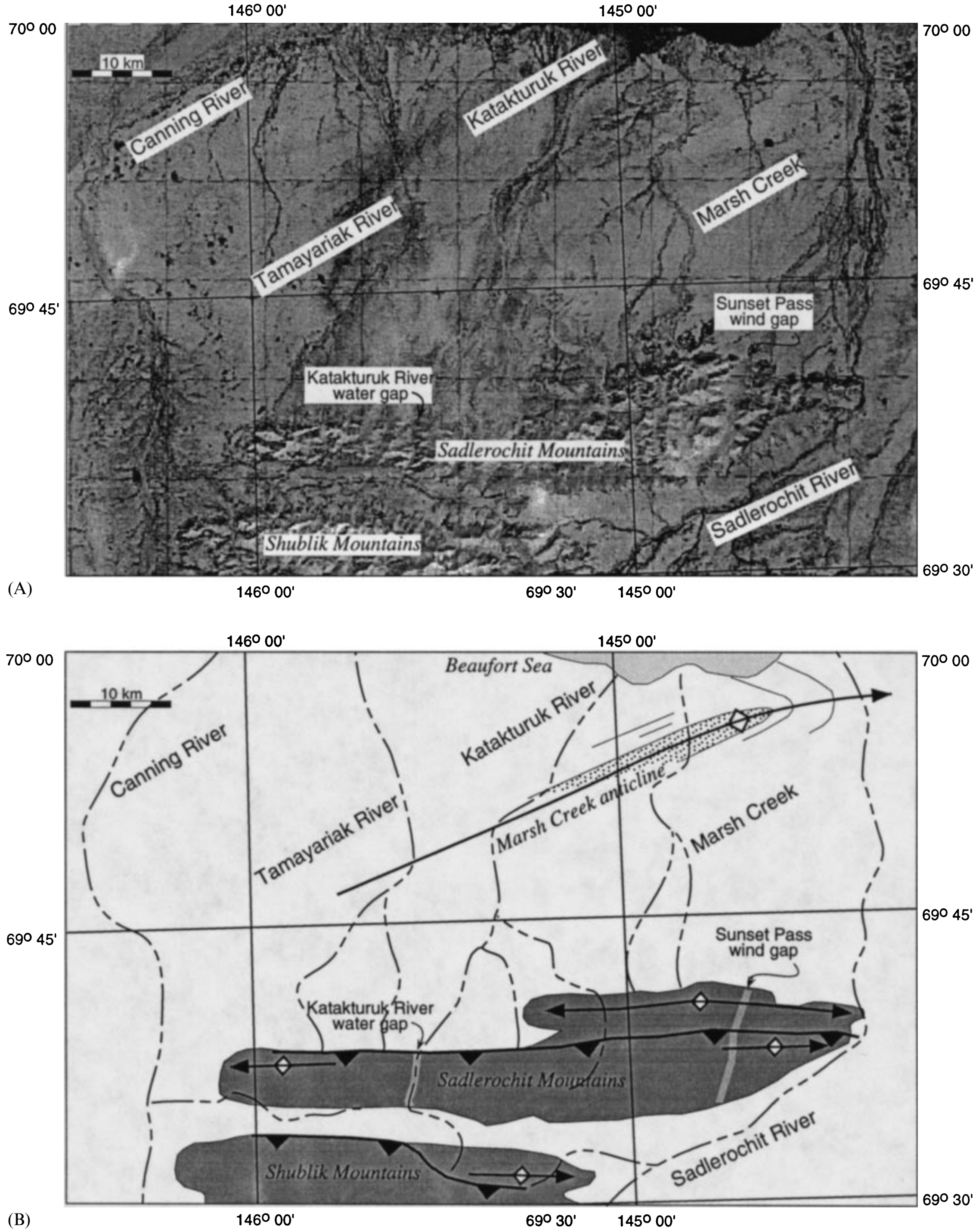

Fig. 13. Satellite image (A) and interpretive map (B) of a portion of the Mt Michelson 1:250 000 quadrangle in the north-eastern Brooks Range. Geology compiled from Bader & Bird (1986), Meigs (1990) and Rogers (1989). Wind gaps, water gaps and deflected streams result from interactions of the regional drainage system with growing folds and faults.

rate and bedrock resistance are approximately constant through time, then, as the zone of uplift broadens, aggradation should occur in the piggyback basin south of the uplift (Figs 11 and 12). As at Wheeler Ridge, this could eventually lead to avulsion out of the wind gap and capture by a lower drainage to the east. Satellite images reveal glacial moraines both east and south of the terminus of the uplifted zone and suggest another potential cause of diversion. These glaciers flowed northward out of the Brooks Range, and it is quite possible that they physically blocked or diverted the Sadlerochit River along their margins, away from its previous course through the wind gap, and into its present position. Thus, although variations in bedrock resistance or the width of the uplift appear unimportant in controlling the diversion, no clear choice can be made among the other options without better control on the history of aggradation in the piggyback basin, discharge changes, contrasts in sediment loads and glacial variations.

ANCIENT FOLDS AND FAULTS AND COEVAL DEPOSITION

Studies of modern growing folds permit geomorphological processes and responses in deforming terrains to be examined in considerable detail. The temporal evolution of the geomorphology and fluvial systems associated with folds, however, is often best reconstructed through the use of subsurface information. In modern settings, seismic and/or drill-hole data can provide some insights on fold evolution and related geomorphological systems. Steeply dipping beds, such as those on fold forelimbs, and stratigraphic data at the scale of individual strata or small groups of strata are, however, difficult to resolve with most seismic data. Typically, these features can be examined in more detail in ancient folds and related syntectonic strata. When folds are well exposed in cross-section and are associated with well-preserved growth strata (Suppe *et al.*, 1992; Vergés *et al.,* 1996), it is possible to reconstruct the history and style of folding and to test whether several folds developed synchronously or in a series of discrete events. In addition, the regional evolution of drainage systems in response to changes in the style and/or rate of deformation can be analysed.

In comparison with modern settings, however, there are several common disadvantages in studying ancient folds. It is usually impossible to document each individual fluvial system or to determine the geometry of their catchments. It is difficult to define many geomorphological parameters such as discharge, stream power or slope. Even when high-quality, three-dimensional exposures are available, it is usually impossible to define reliably all of the coexisting river patterns or to reconstruct even a single, complete fluvial system at one specific time.

Nonetheless, well-preserved ancient strata can provide a complementary perspective to that derived from the examination of modern folds. Here, we describe a well-exposed region of folds, faults and syndeformational strata in north-eastern Spain, where we have mapped large-scale bedding geometries and thickness variations in order to define the successive development of several folds. In this same area, cross-cutting relationships among alluvial strata and thrust faults and localized variations in the depositional regime are used to constrain the behaviour of faults that cut the former land surface, whereas unconformities, onlapping stratal geometries and karstified landscapes have been used to reconstruct palaeotopography and palaeovalleys. Finally, the overall geometry of the regional depositional system during fold growth has been examined on the basis of >1500 palaeocurrent measurements collected from furrowed bases of conglomerates and from clast imbrications. This study area in the Catalan Coastal Range provides clear stratigraphic evidence for the synchronous growth of two elongate folds with limbs that underwent major rotation during folding. Throughout much of the fold growth, depositional rates outpaced crestal uplift rates, such that rivers flowed across the fold crests. Palaeovalleys and palaeotopography strongly influenced early drainage development, and there is clear evidence for thrust faults that cut the depositional surface and influenced local deposition.

Peñagalera Conglomerate, NE Spain

Geological setting

The south-eastern margin of the Ebro Basin in Spain (Fig. 14) is delineated by the Catalan Coastal Ranges which, during Eocene and Oligocene times, were the hinterland source areas for coarse-grained alluvial fans that were shed into the Ebro Basin (Anadon *et al.,* 1986; Colombo & Vergés, 1992). The hinterland in the SW part of the range consists primarily of Mesozoic carbonates strata that have been imbricated by numerous NE-striking, NW-vergent thrust faults. A regionally important decollement level is localized in Triassic evaporites (Domingo & Olmedo, 1985; Roca, 1992). Most of the contractional deformation occurred during Palaeogene times due to the convergence of the Iberian peninsula with south-western France.

The study area lies 150 km WSW of Barcelona near Beceite and Arnés along the interface between the thrusted pretectonic carbonate strata of the SW Catalan Coastal Ranges and the alluvial apron of the adjacent Ebro foreland (Fig. 15). Palaeogene conglomerates are folded into an elongate syncline that stretches for 18 km parallel to the thrust front. The syncline's south-east limb is commonly vertical to overturned adjacent to the exposed pretectonic strata, comprising primarily Mesozoic carbonates (Figs 15 and 16). A complex suite of anticlines and thrusted anticlines in these carbonates abuts the proximal, south-eastern limb of the conglomeratic syncline. The syncline itself is ≈ 1.5–2 km wide. An anticline to the north-west of the syncline, with which it shares a common limb and parallel trend, has variable structural relief along its length. A structural saddle midway along the anticline's length indicates the zone of least structural relief. Progressing from this saddle toward the SW, the anticline evolves from a largely symmetrical fold with limbs dipping $<45^\circ$ into a strongly asymmetric fold with an overturned north-western limb (Fig. 16). Prefolding Palaeogene strata are exposed in the core of the anticline along most of its length. Still further toward

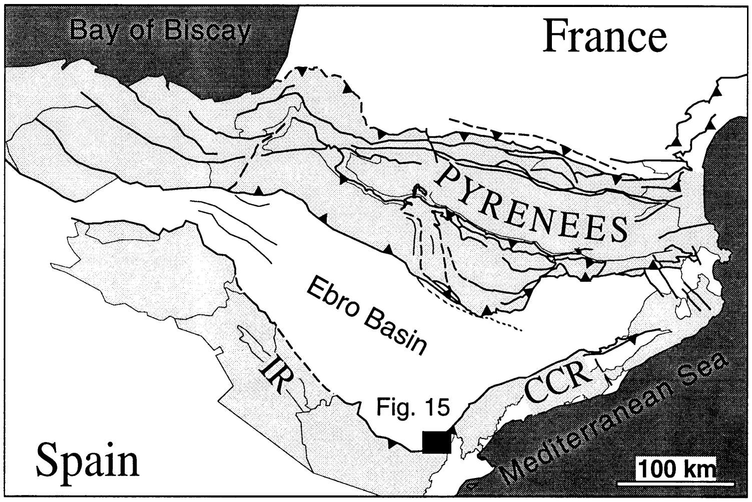

Fig. 14. Simplified geological map of north-eastern Spain, showing Ebro foreland basin, Pyrenees, Iberian Range (IR) and the Catalan Coastal Ranges (CCR). Box indicates location of study area. Map based on Vergés (1993).

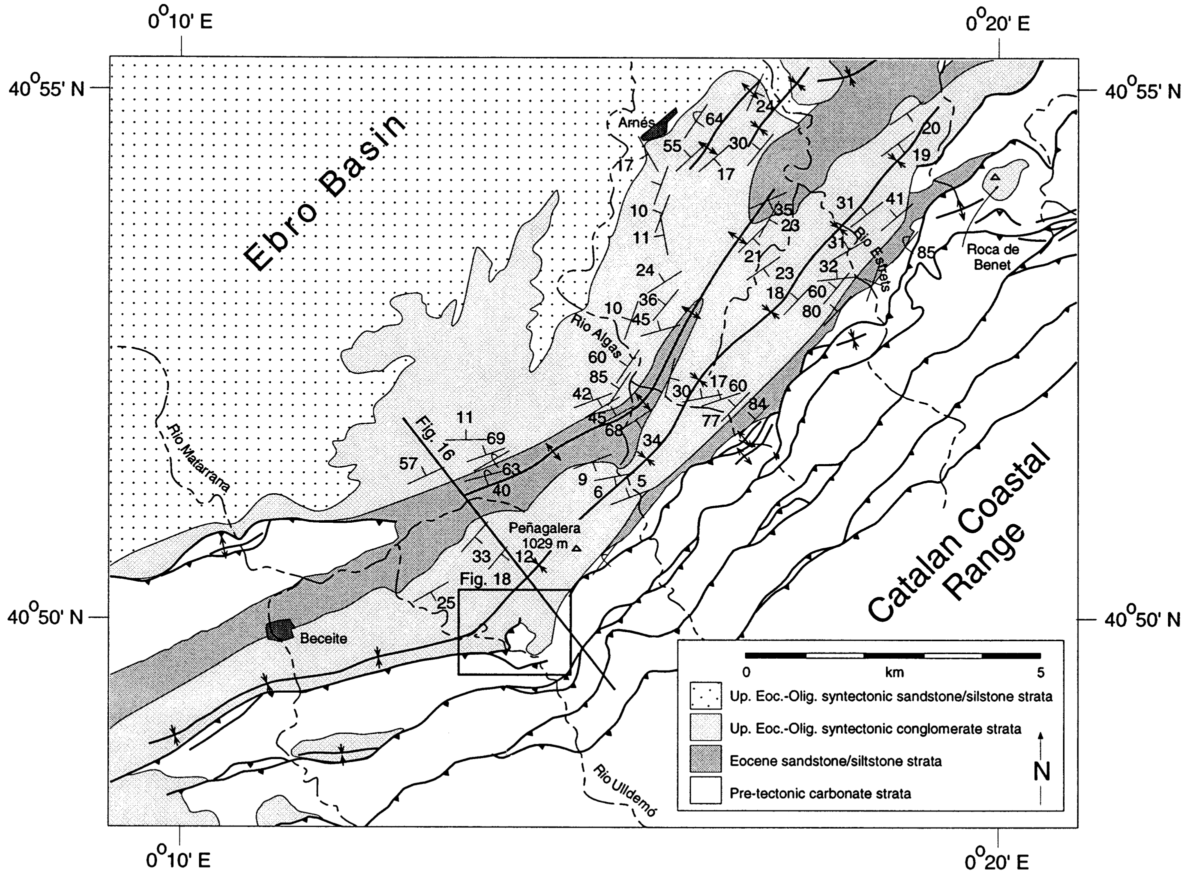

Fig. 15. Simplified geological map of study area in the south-western Catalan Coastal Ranges, showing Peñagalera, Beceite, large-scale structures and major rivers. This study focuses on the growth synclines parallel to the folded and thrusted hinterland which comprises predominantly carbonate thrusts sheets.

the SW, the anticline attains its maximal structural relief in the hangingwall of an emergent, NW-vergent thrust involving Triassic and younger strata near Beceite (Fig. 15). Several small rivers exit the thrusted hinterland at high angles to the trends of the thrusts (sites a–e, Fig. 17b). In most places, their entrance into the foreland coincides with a structural re-entrant, rather than with a salient, or they occur along an apparent zone of wrench faulting where displacement is transferred to a more forelandward thrust fault.

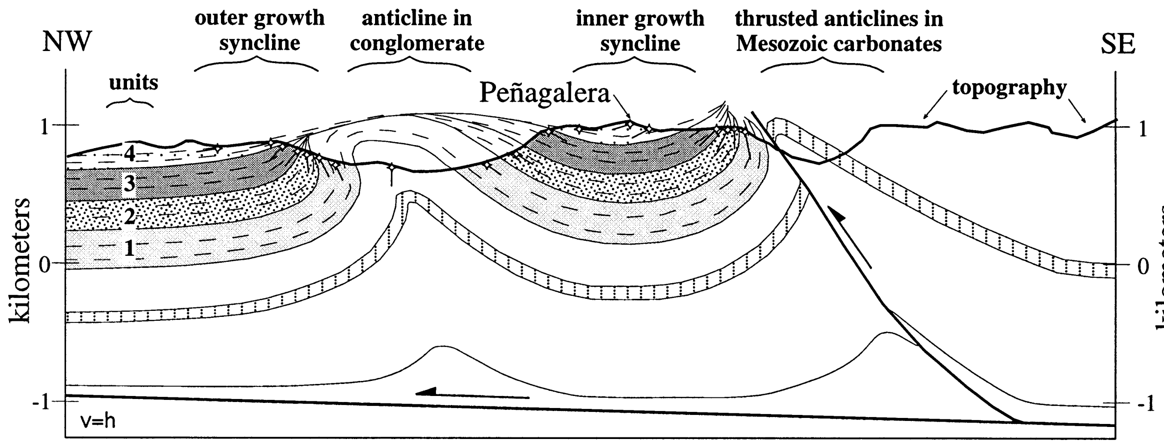

Fig. 16. Simplified cross-section near Peñagalera showing two growth synclines and the interpretation of buckle folds underlying the intact and breached anticline. Note strong overturning of the forelimbs of the folds and the constant thickness of unit 1 across the central anticline. This indicates that growth of this anticline began after deposition of unit 1. See Fig. 15 for location.

Nature of folding

Extensive exposures of syntectonic strata permit the sequence and style of folding to be clearly defined in much of the study area. Within the south-east limb of the syncline and the north-west limb of the anticline within the conglomerates, Palaeogene alluvial strata display a progressive rotation and steepening of bedding toward the south-east (Figs 15 and 16). Where beds can be traced from the core of the syncline toward its margins, the individual beds and groups of beds can be shown to thin toward the south-eastern limb of the syncline. The stratal rotation and bed thinning are consistent with growth folding: deposition was synchronous with folding and systematic changes in bedding thicknesses are primarily due to differential folding (Suppe *et al.*, 1992) that caused accommodation space to vary on a scale commensurate with that of the wavelength of the folds. Correlation of differentially rotated synclinal strata across the intervening anticline provides clear evidence for synchronous growth of both folds (Fig. 16). Thus, for at least part of the Palaeogene deposition, serial folding occurred adjacent to the thrusted basin margin.

During the initial stages of deformation, however, it appears that the south-eastern (proximal) folds in the Mesozoic carbonate strata began to develop prior to the outer, distal fold. Whereas the basal conglomeratic unit (unit 1, Fig. 16) shows clear evidence for syndepositional rotation where it abuts the hinterland to the south-east, it displays uniform thicknesses on both flanks of the anticline. Moreover, there is little variation in stratal dips within unit 1 on either limb of the anticline, although there are strong dip contrasts between the limbs. This consistency in thickness between limbs and in dip within limbs argues against any rotation or uplift of this anticline during deposition of unit 1.

On the distal, north-western flank of the anticline, the younger conglomeratic strata (units 2–4; Fig. 16) display a clear fanning of dips and provide unambiguous evidence for fold growth during deposition. Equivalent strata on the south-eastern limb of the anticline display only a minor rotation. This contrast between the rotation recorded by the two limbs is instructive, because both limbs experienced the same crestal uplift of the intervening anticline. Differential rotation appears to be a result of the asymmetric shape of the fold (overturned forelimb vs. gentle backlimb) and the proximity of the preserved strata to the fold crest. The less differentially tilted strata to the south-east are both on a gentler limb and further from the fold crest (Fig. 16). Near the axis of the growth syncline, little or no rotation would be expected (Fig. 6).

The youngest preserved conglomeratic strata are moderately tilted in most localities. Within the resolution of this poorly dated succession therefore synchronous folding of these parallel structures persisted until the end of recorded deposition. Projections of differentially tilted conglomeratic bedding across the anticlinal crest indicate that $\approx$400–500 m of erosion of the crestal region occurred during folding (Fig. 16). All of this erosion represents bevelling of apparently weakly cemented, syntectonic conglomerates as they were lifted above the local base level and were intersected by transverse rivers.

There is no unique solution for the underlying structure of the cross-section (Fig. 16). Detachment folding could generate the observed fold geometries (Jamison, 1992; Epard & Groshong, 1993; Hardy & Poblet, 1994; Homza & Wallace, 1995) and would be consistent with the mobility of the Triassic strata which appear to occupy the core of the folds (Domingo & Olmedo, 1985). Alternatively, the core of the folds could comprise an imbricated stack of thin thrust sheets. This could be considered consistent with the style of thrust imbrication that is seen within the Catalan Coastal Ranges to the south-east (Fig. 15) of this study area (Domingo & Olmedo, 1985). Both models could explain the strong forelimb rotation that is observed. We choose here the detachment-fold geometry for its simplicity and its simi-

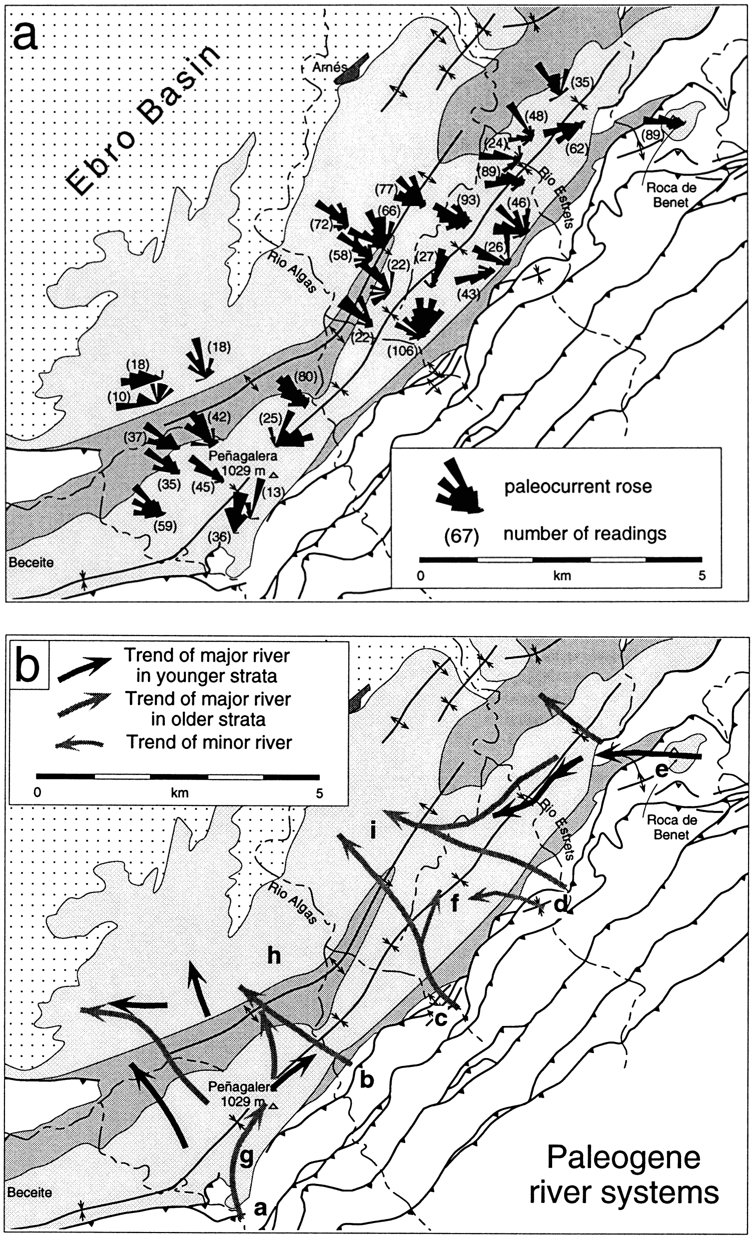

Fig. 17. (a) Palaeocurrent directions (> 1500 measurements) between Peñagalera and La Roca de Benet. About 80% of the measurements in each palaeocurrent rose represent orientations of furrows on the bases of large conglomeratic beds. The remaining directions are based on clast imbrications and cross-beds. Largely transverse drainage dominates the region, despite active folding during deposition. Most deviations from the transverse pattern appear to represent either flow into interfan areas between major drainages, the influence of palaeochannels or moderate deflection of rivers by the growing anticline. (b) Interpretation of palaeocurrent roses. Major drainages enter the foreland at sites a–e and are associated with re-entrants and zones of wrench faulting. A bajada of conglomeratic, transverse fans dominates the proximal area. Convergent flow at site f suggests an interfan zone. Flow in the central region is consistently transverse across the anticline in the foreland and appears focused in the structural saddle near site i and near site h. In the Rio Ulldemó re-entrant (site a), a palaeovalley (site g) re-directs flow to the north until the valley is filled and rivers flow directly to the north-west. Palaeocurrents in the youngest units < 1 km north of Peñagalera appear be deflected by the growing anticline.

larity to many other folds in north-eastern Spain (Anadon *et al.*, 1986; Vergés, 1993).

Depositional response to concurrent folding

Given the amplitude and sequence of fold development as determined from the syntectonic strata, it is possible to investigate how the fluvial system interacted with the growing folds. Based on more than 1500 palaeocurrent measurements collected from an array of > 30 sites, syntectonic deposition appears to have been dominated by transverse fluvial systems that flowed to the north-west (Fig. 17). In general, little deflection of drainages is apparent across the crest of the anticline and, with few exceptions, the flow directions are nearly orthogonal to the regional structure. Although the observation that rivers appear to have flowed unperturbed across the anticlinal crest would often be interpreted to suggest that the accumulation rate exceeded the crestal uplift rate (Fig. 3 or 2), the specific cross-section here (Fig. 16), in combination with the palaeocurrent data, suggests that the fold crest was simply eroded as it was uplifted (Burbank & Beck, 1991). Therefore, rivers were able to traverse it without significant obstruction, but the rate of structural uplift of the fold would have exceeded the rate of aggradation along its limbs. We cannot test the possibility that water gaps existed across the crest of the anticline because the contact between the pre- and syntectonic strata is not preserved along most parts of the fold crest.

The most abundant palaeocurrent data come from the inner growth syncline which is dominated by transverse palaeocurrents in its central and south-western parts. In the north-east, there is a substantial component of westward flow, oblique to the synclinal axis. These oblique directions suggest that the river exiting the hinterland near the Roca de Benet (site e, Fig. 17) was commonly deflected toward the south-west by the rising anticline in its path toward the foreland. In the proximal syncline between the Rio Estrets and the Rio de les Valls, there appears to be convergent flow. If the past positions of these rivers as they emerge from the hinterland were similar to those of today, the region of convergent flow could be interpreted as an interfan region which lay between two larger fans with radii of 1–2 km (site f on Fig. 17).

Due to poorer exposures and gentler tilting of the north-western limb of the outer anticline, there are fewer palaeocurrent data presently available from this fold. Nonetheless, the data are consistent with transverse flow across at least the central part of this fold (Fig. 17). Unlike the inner syncline which is uniformly dominated by conglomerates and appears to represent an ancient bajada, considerable lateral facies variability characterizes the north-western limb of the outer anticline. Thick conglomerate bodies appear to be concentrated in a few discrete zones (sites h and i, Fig. 17), whereas interbedded sandstone and overbank deposits are more abundant in the intervening areas. Thus, although transverse palaeocurrents dominate the bajada of the internal growth syncline, the main rivers appear to have been more focused by the time they crossed the outer syncline. This focusing is interpreted to have two causes. First, focusing results from partial deflection of some of the tributary rivers (entering from sites a and e, Fig. 17) as they approached the rising anticline. Second, near the structural saddle (between sites f and i, Fig. 17), uniform dips through nearly all of the exposed conglomerates on each side of the anticline indicate that the anticline grew here near the end of deposition. Thus, it was a structural low during most of the depositional history recorded here. Lateral propagation of the adjacent anticlines towards this saddle would tend to deflect flow into it. In contrast to the individual rivers entering the foreland or to rivers whose catchments lay exclusively within the proximal foreland, the major rivers crossing the anticline would have had higher discharges, and conglomerates should have prograded further along the courses of these focused rivers.

Palaeovalleys

An illustrative example of a palaeovalley and its influence on drainage patterns can be found in the SW quadrant of the study area. At present, the Rio Ulldemó emerges into the foreland through a structural re-entrant south of Peñagalera (site a, Fig. 17). A pronounced, N–S-orientated growth syncline with an overturned proximal limb is present along the boundary between the Palaeogene conglomerates and the hinterland thrust sheets and folds (Fig. 16). The distal, western limb of this syncline is defined in its lower part by a wall of Mesozoic carbonate strata against which the syntectonic conglomerates onlap (Fig. 18). Although the contact between the carbonates and the conglomerates is not exposed along its full length, the upper 50 m of the exposure reveals a buttress unconformity where conglomeratic strata abruptly abut the carbonates along a highly discordant contact. Carbonate breccias derived from the nearby bedrock are preserved along the onlap contact. Whereas the contact itself dips steeply, the conglomerate beds dip gently toward the contact and clearly indicate that the wall of carbonates represented palaeorelief which was progressively onlapped by the aggrading syntectonic conglomerates. Hence, this defines the western margin of a palaeovalley. The topmost contact of the Mesozoic carbonates is an undulating surface overlain by ≈ 100 m of younger, subhorizontal conglomerate (unit 4, Fig. 18). This gently inclined depositional contact provides additional evidence for palaeorelief during the early stages of syntectonic deposition, because it fossilizes a karstic weathered zone on the carbonates. Depressions ≈ 10 m deep and filled with locally derived breccias are found along the upper surface of the carbonate. We interpret these solution features and breccias to have developed when the carbonate strata stood in isolated relief above the adjacent landscape (Fig. 19).

Palaeocurrents along the northern projection of the palaeovalley are orientated to the north (Fig. 17). Other than the interfluve–interfan regions previously described, this is one of the few places within the study area where the observed palaeoflow in a proximal locality is not transverse to the mountain front. The oblique diversion of flow is interpreted to result from channellization by the palaeovalley through remnant topography that had been etched in the pretectonic strata prior to conglomeratic deposition. This flow is interpreted to turn to the north-west as it joined a larger river near the present course of the Rio Algas. When the palaeovalley was overtopped by unit 4 (Fig. 18), flow appears to have become more north-westerly (Fig. 17b), directly out of the re-entrant. Any flow to the north would have been diminished, which may account for the flow directions parallel to the synclinal axis in the youngest strata north of Peñagalera: due to diminished stream power, the river was no longer able to bevel the rising anticline and was deflected parallel to it. Similar palaeovalleys and flow diversion have been documented in syntectonic conglomerates of the Pyrenees (Burbank & Vergés, 1994).

Due to cover within the growth syncline, bedding geometries and contact relationships along the palaeovalley wall cannot be fully documented. Conglomeratic strata that are abruptly folded near the contact with the carbonates attest to later folding of both walls of the palaeovalley. Pronounced unconformities and strong differential rotation of strata within the growth syncline indicate that considerable horizontal shortening occurred

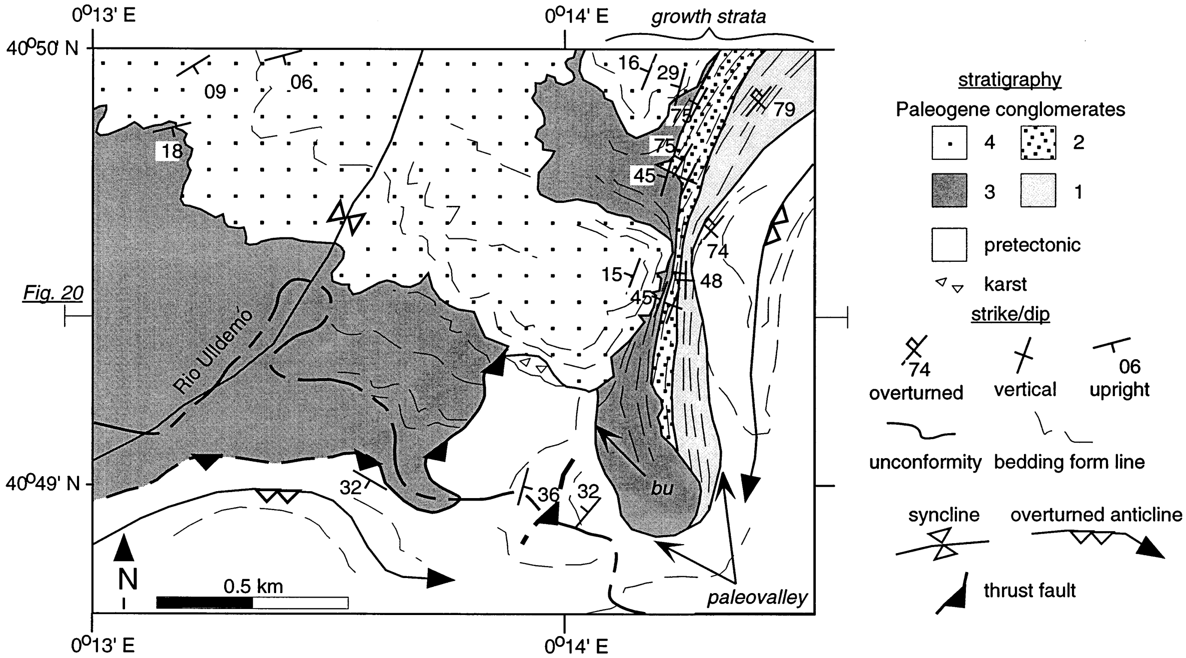

Fig. 18. Simplified geological map of the Rio Ulldemó re-entrant, including a palaeovalley bounded by a buttress unconformity on its western margin. Abrupt rotation of units 1–3 adjacent to the hinterland defines a strongly deformed growth syncline. The north-trending thrust cuts unit 3 and the base of unit 4. Map based on field data and photographic interpretation.

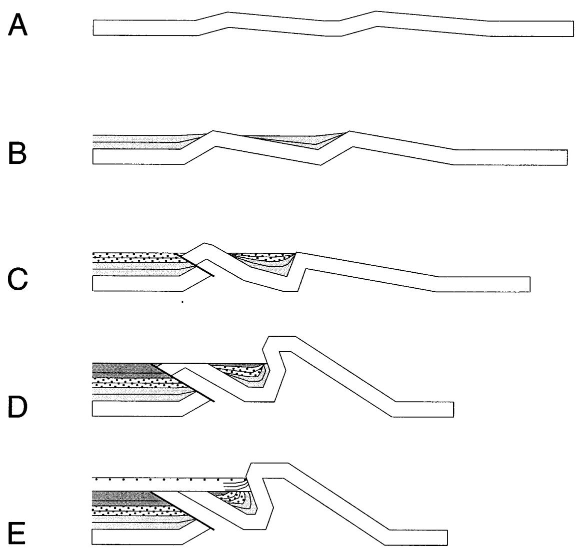

Fig. 19. Schematic sequential evolution of folds, thrust and growth strata in the Rio Ulldemó re-entrant. The right-hand growth syncline (steps B–E) continuously deforms, as the fold amplitude increases and the syncline tightens due to strong translation of the anticline. Angular unconformities bound each of the syntectonic units in the syncline. The thrust fault cuts a second anticline and transports the right-hand growth syncline in its hangingwall. Thrusting is coeval with deposition of units 2 and 3, but wanes and is overlapped by unit 4. For location of section, see Fig. 18.

during deposition (Vergés *et al.*, 1996). Much of this shortening was driven by westward transport of the overturned anticline in the carbonate strata that bounds the eastern margin of the growth syncline. At the same time, unless the carbonates which delineate the buttress unconformity created >200 m of palaeorelief above the floor of the palaeovalley at the initiation of conglomeratic deposition, this distal wall of the growth syncline must also have been rising above an active fold or fault.

Thrust faults at the surface

Whereas some of the faulting in this study area can be shown to post-date deposition, at least one active thrust fault consistently cut the surface during most of its activity. In the Rio Ulldemó re-entrant, the carbonate strata which constitute the western wall of the palaeovalley are truncated further to the west by a thrust fault (Fig. 18). Traceable from the modern valley bottom, the thrust fault is exposed as a nearly planar surface that dips ≈ 30–35° to the east-south-east and delimits the western edge of the exposed pre-Cenozoic bedrock in this re-entrant. Large carbonate boulders and locally derived breccias are preserved in the nearly horizontal conglomerate strata that are cut by the thrust. The presence of these sedimentary breccias indicates that the carbonate rocks in the hangingwall were exposed at the surface during thrusting (Fig. 7). It appears therefore that the conglomerates were simultaneously aggrading and being cut by the active thrust, and it seems likely that the rates of aggradation and vertical uplift of the hangingwall were comparable. At the thrust's uppermost extent, ≈ 200 m above the valley bottom, it clearly offsets the basal conglomeratic beds that overlapped the carbonate strata of the hangingwall. Thus, even as the rate of aggradation began to exceed the rate of thrusting and uplift, newly overlapping strata were cut by the thrust (Fig. 18). Along the upsection projection of the thrust, several additional conglomerate beds are folded with the same sense offset as seen on the thrust. These strata thicken across the fault projection, whereas still younger beds cross its projection without apparent deflection or thickening: these clearly record the termination of thrust motion.

Synchronous folding, faulting, and deposition

Bedding geometries, depositional patterns and cross-cutting relationships in the Rio Ulldemó re-entrant (Figs 18 and 19) clearly demonstrate one way in which syntectonic strata can be used to document synchronous development of multiple structures. Less than 1 km to the north, the cross-section (Fig. 16) illustrates the coeval development of two growth synclines whose axes are ≈ 3 km apart. Within the re-entrant itself, synchronous growth folding and thrust faulting at the surface (Fig. 19) is recorded by units 2 and 3 (Fig. 18). In the eastern growth syncline, both units are bounded by unconformities, and there is a fanning of dips within each: these clearly result from folding due to growth of the anticline to the east (Fig. 19). Moreover, the observation that the unconformities are not limited to the proximal part of the growth syncline (as is typical in many other folds: Fig. 6) indicates erosion cut deeply into the distal part of the syncline as the forelimb steepened and became overturned. At this time, the rate of aggradation was clearly slow with respect to the rate of crestal uplift and forelimb rotation. To the west <1 km, unit 3 (and possibly unit 2) is cut by the thrust fault described above. The thrust is also interpreted to cut an underlying fold in the pretectonic strata (Fig. 19). Some of this folding may have been inherited from an earlier deformational episode, because the subhorizontal, karstic upper surface of the thrust's hangingwall suggests weathering of a palaeohigh during (and possibly prior to) the early stages of deposition. This surface was passively lifted above the thrust ramp until it was overlapped by conglomerates as thrusting waned (Figs 18 and 19). Along the line of section, but 2 km further west, the growth of the major anticline also affected units 2–4 (Fig. 16). In the spatially restricted Rio Ulldemó re-entrant therefore syntectonic sediments clearly demonstrate that two folds and an intervening thrust were all active simultaneously during deposition of unit 3.

DISCUSSION

Even when there is a clear conceptual understanding of the ways in which depositional and erosional processes may interact with growing structures, the multiplicity of independent, competing and often hard-to-calibrate variables often makes it difficult to resolve unambiguously the factors that control observed geomorphological or geological conditions. Is it accelerated rates of crestal uplift, enhanced rates of sediment supply from the hinterland, increasing resistance to erosion of the substrate or climatically controlled changes in discharge and stream power that cause a formerly antecedent river to be defeated? Often, it is impossible to calibrate these variables in absolute terms. For example, reconstruction of changes in elevation above an assumed 'fixed' datum, such as sea level or the geoid, is notoriously difficult in terrestrial settings (England & Molnar, 1990; Molnar & England, 1990; Gregory, 1994). Similarly, even if good-quality time control is available, the details of sediment-accumulation rates are hard to determine because of the discontinuous time series represented by the chronological data (Badgley *et al.,* 1986; Talling & Burbank, 1993), the unknown temporal gaps represented by each bedding contact (Sadler, 1981; McRae, 1990), and the unknown history of cementation, dissolution and compaction that have affected preserved thicknesses following deposition (Sclater & Christie, 1980; Guidish *et al.,* 1985; Gallagher, 1989).

Although absolute calibration of individual variables is desirable, the relative rates or magnitude of competing sets of variables can sometimes yield key insights into changes in these ratios through time and into the probable impact of these changes. The relative rate of sediment accumulation vs. crestal uplift can be clearly recorded by growth strata (Suppe *et al.*, 1992; Burbank & Vergés, 1994). This ratio reveals whether a growing feature would have had a topographic expression, whether or not an antecedent river would have had to bevel off the crest of the structure in order to continue flowing across it and whether onlapping or offlapping geometries should be preserved on the fold limbs (Burbank & Vergés, 1994). If even a single variable can be well understood, it can place definite limits on permissible interpretations. For example, water discharge is a key determinant of stream power. If it can be shown through observations of cross-sectional channel and bedding geometries (Willis, 1993) that the palaeodischarge of a river did not change significantly during the interval of interest, then the defeat of that river by a growing fold cannot be attributed to a climatically modulated reduction in stream power or to river capture. On the other hand, calculations of palaeoslopes (Heller & Paola, 1989) are still sufficiently imprecise that changes in stream power due to gradient adjustments are usually impossible to resolve.

In some modern geomorphological situations, the ergodic hypothesis (in which space is substituted for time) can be used to analyse likely changes and responses in the past. At Wheeler Ridge, for example, it appears that the structure has grown through gradual propagation to the east (Medwedeff, 1992). Given the ages for the abandoned fluvial surfaces that form the crest of each segment of the fold (Keller *et al.,* Zepeda *et al.,* 1990), the timing of this propagation and initial uplift of the fold crest above the adjacent plain can be reconstructed. The eastern part of Wheeler Ridge can be studied as an analogue for geomorphological responses to an initial uplift of a fold above base level, whereas the western part provides an analogue for changes that are likely to occur in the newly emergent part of the fold as it evolves geometrically and geomorphologically. Based on digitized topography, the surficial characteristics of growing folds can be quantified and compared along strike to investigate correlations between different facets of this geomorphological system, such as those between fan size and the slope and relief of contributing areas. These relationships can then form a basis for quantitative predictions of future changes in the surface of the fold and the surrounding landscape. Unless one has a clear understanding of (1) the subsurface geometry of the beds, (2) changes in discharge, slope and bedrock resistance and (3) rates of accumulation, uplift, subsidence or sediment supply through time, one often can only speculate about the long-term geometric evolution of a fold and the causes of defeat and deflection of formerly antecedent rivers, despite improved understanding of processes and responses in present landscapes. When space can be substituted for time along a growing structure, however, past and future changes in the geomorphological system can be better understood and predicted.

The data in this study indicate that even the growth of folds with several hundreds of metres of relief does not necessarily force rivers to reorganize. The rate and geometry of fold growth, the resistance of the bedrock, rates of aggradation and specific stream power determine how antecedent rivers will respond to uplifts along their courses. A simple geometric model, described here and supported by topographic data from Wheeler Ridge, indicates that aggradation within a piggyback behind a growing fold could readily lead to defeat of an antecedent stream, irrespective of other changes in stream power, resistance or uplift rate. Many piggyback basins display an asymmetrical structural geometry, such that they are open at one end and are closed by overlapping thrusts or folds at the other end. In this situation, almost any river deflected by a growing structure must eventually flow towards the open end of the piggyback basin. The plunging noses of most growing folds propagate laterally through time. Whenever a formerly antecedent river is defeated by a growing and laterally propagating fold, its catchment area and discharge will increase as it is deflected toward the open end of a piggyback basin. Thus, the probability of maintaining an antecedent course across a growing fold increases toward the nose of a propagating fold, because increasing amounts of discharge and the potential for greater stream power characterize these rivers.

Limited exposures of growth strata adjacent to ancient folds and post-depositional modification of these strata, however, typically preclude complete three-dimensional description of any former landscape. Even in arid localities without vegetative cover, erosion has usually removed the stratigraphic evidence of at least some key relationships. Nonetheless, detailed field observations of ancient folds and related growth strata can permit sequential reconstructions of an evolving depositional system in an actively deforming environment. Data on folds, faults and palaeotopographic configurations in pretectonic strata and on palaeocurrents, stratal geometries and sedimentary facies preserved in syntectonic strata can be used to assess the competition between geomorphological, sedimentological and tectonic controls on ancient landscapes as they evolve through time.

Analysis of the geomorphology of the Wheeler Ridge fold and conceptual models related to the defeat of formerly antecedent rivers have some important implications for the analysis of fluvial patterns in ancient piggyback basins. In general, piggyback basins will have depositional surfaces which slope toward an outer emergent structure and toward the open end of the piggyback basin. Often the bounding structure is also propagating in this direction. When an antecedent river is defeated by a growing anticline, its new course will be controlled by these slopes within the piggyback basin. Therefore, its deflected course will generally be parallel and adjacent to the outer, bounding structure. In the stratigraphic record, unfortunately, it is these strata immediately adjacent to a structure that are often removed during subsequent uplift and erosion. Consequently, the deflected course of a defeated antecedent river may not be recorded. In contrast, strata in the middle of the piggyback basin have a higher preservation potential. These strata may indicate that the river in the piggyback basin was flowing directly toward the outer, bounding structure, thereby suggesting that an antecedent river persisted across this structure. In such a scenario, the stratal record on the distal flank of the bounding structure becomes very important, because here it may be possible to document changes in provenance or channel size and style which would indicate a contrast between the defeated river in the piggyback basin and the smaller rivers with local catchments on the distal flank of the structure.

CONCLUSIONS

A dynamic interplay between growing folds and coexisting fluvial systems results from the interactions of competing variables. Simple conceptual models suggest that, when the rate of aggradation exceeds the rate of crestal uplift of a fold, rivers will flow without impedance across the fold. When a fold develops a topographic expression at the surface, the persistence of a river across the structure is facilitated by high stream power, high rates of aggradation, low rates of hinterland sediment supply, low rates of crestal uplift, small fold wavelengths, readily eroded rocks in the core of the fold and the presence of transverse structures. Within piggyback basins, deposition is caused by local base-level rises and gentler fluvial gradients resulting from folding. Aggradation in piggyback basins generates topographic slopes that can favour avulsion, stream capture and defeat of antecedent rivers. Digital topographic data permit ready quantification of some landscape characteristics related to stream patterns, such as the magnitude and pattern of uplift, river gradients, floodplain slopes and likely zones of aggradation or incision. When combined with a model for fold growth and with chronological data, the geomorphological modification of a growing fold can be examined based on calibrated rates of erosion, river incision and sediment production. In ancient rocks, the key to reconstructing the interactions of folds and rivers is the study of growth strata which can reveal the sequencing of folding events, demonstrate synchronous development of multiple folds and record the response of rivers to these growing folds.

Improved comprehension of landscape evolution in actively deforming regions will emerge from studies which combine analysis of both ancient and modern examples in similar tectonic settings. Determination of absolute rates through dating of as many stratigraphic, geomorphological and structural events as possible permits a quantification of temporal changes in variables that control depositional systems. Reliable temporal calibration also permits direct comparison with related data sets, such as chronological data regarding climatic change or specific tectonic events. Calculation of relative rates of processes is often possible and instructive, even if absolute time control is missing. Excavations (Sieh *et al.*, 1989) and high-resolution, shallow seismic data (Alexander *et al.*, 1994) can begin to reveal the three-dimensional changes through time in modern settings, but considerably longer, detailed records spanning several climatic cycles and a long history of deformation are typically only available through stratigraphic studies. Whereas in both modern and ancient settings the record of geomorphological and structural change will always be incompletely known, field observation and calibration of features representing as many of the key variables as possible will permit improved evaluation of the controls on landscape change and will facilitate the development and testing of improved conceptual and quantitative models.

ACKNOWLEDGEMENTS

This research was supported by grants from the NSF (EAR-9220056, 9218645, 9304863), NASA (NAGW-3762) and by the donors of the Petroleum Research Fund (ACS-PRF 17625, 23881). Field assistance and helpful discussions in Spain with J. Vergés, J. Friedmann and P. Hogan are gratefully acknowledged. Eric Fielding contributed significantly to the analysis of the digital topography. Reviews by John Crowell and Frank Pazzaglia significantly improved this manuscript. This analysis was enhanced by an educational grant from Earth Resource Mapping and by a graphics tower donated by Sun Microsystems.

REFERENCES

Alexander, J., Bridge., J.S., Leeder, M.R., Collier, R.E.L. & Gawthorpe, R.L. (1994) Holocene meander-belt evolution in an active extensional basin, southwestern Montana. *J. Sed. Res.*, **B64**, 542–559.

Anadon, P., Cabrera, L., Colombo, F., Marzo, M. & Riba, O. (1986) Syntectonic intraformational unconformities in alluvial fan deposits, eastern Ebro Basin margins (NE Spain). In: *Foreland Basins* (Ed. by P. A. Allen and, P. Homewood), pp. 259–271. Blackwell Scientific Publications, Oxford.

Bader, J.W. & Bird, K.J., (1986) Geologic map of the Demarcation Point, Mt. Michelson, Flaxman Island, and Barter Island quadrangles, Northeastern Alaska. *U.S. Geol. Surv. Map 1–1791.*

Badgley, C., Tauxe, L. & Bookstein, F. (1986) Estimating the error in age interpolation in sedimentary rocks. *Nature*, **319**, 139–141.

Beaumont, C., Fullsack, P. & Hamilton, J. (1992) Erosional control of active compressional orogens. In: *Thrust Tectonics* (Ed. by K. R. McClay), pp. 1–18. Chapman and Hall, London.

Bull, W.B. (1991) *Geomorphic Responses to Climatic Change*. Oxford University Press, Oxford.

Burbank, D.W. & Beck, R.A. (1991) Rapid, long-term rates of denudation. *Geology*, **19**, 1169–1172.

Burbank, D.W. & Raynolds, R.G.H. (1988) Stratigraphic keys of the timing of thrusting in terrestrial foreland basins: applications to the northwestern Himalaya. In: *New Perspectives in Basin Analysis* (Ed. by K. L. Kleinspehn and C. Paola), pp. 331–351. Springer-Verlag, New York.

Burbank, D.W. (1992) Causes of recent Himalayan uplift deduced from deposited patterns in the Ganges basin. *Nature*, **357**, 680–682.

Burbank, D.W. & Vergés, J. (1994) Reconstruction of topography and related depositional systems during active thrusting. *J. geophys. Res.*, **99** (20), 281–20, 297.

Burbank, D.W., Vergés, J., Muñoz, J.A. & Bentham, P.A. (1992) Coeval hindward- and forward-imbricating thrusting in the central southern Pyrenees: timing and rates of shortening and deposition. *Bull. geol. Soc. Am.*, **104**, 1–18.

Colombo, F. & Vergés, J. (1992) Geometria del margen S.E. de la Cuenca del Ebro: discordancias progresivas en el Grupo Scala Dei. Serra de La Llena. (Tarragona). *Acta geol. Hisp.*, **27**, 33–53.

Dawers, N.H. & Anders, M.H. (1995) Displacement-length scaling and fault linkage. *J. Struct. Geol.*, **17**, 607–614.

Decelles, P.G., Gray, M.B., Ridgway, K.D., Cole, R.B., Srivastava, P., Pequera, N. & Pivnik, D.A. (1991) Kinematic history of a foreland uplift from Paleocene synorogenic conglomerate, Beartooth Range, Wyoming and Montana. *Bull. geol. Soc. Am.*, **103**, 1458–1475.

Dietrich, W.E., Wilson, C.J., Montgomery, D.R., Mckean, J. & Bauer, R. (1992) Erosion thresholds and land surface morphology. *Geology*, **20**, 675–679.

Dolan, J.F., Sieh, K., Rockwell, T.K., Yeats, R.S., Shaw, J., Suppe, J., Huftile, G.J. & Gath, E.M. (1995) Prospects for larger or more frequent earthquakes in the Los Angeles metropolitan region. *Science*, **267**, 199–205.

Domingo, A.G.D. & Olmedo, F.L. (1985) Mapa Geologico de España: Horta de San Juan, 1:50,000. *Instituto Geologico y Minero de España*, **496**.

Eisbacher, G.H., Carrigy, M.A. & Campbell, R.B. (1974) Paleodrainage pattern and late orogenic basins of the Canadian Cordillera. In: *Tectonics and Sedimentation* (Ed. by W. R. Dickinson), pp. 143–166. Society of Economic Paleontologists and Mineralogists.

England, P. & Molnar, P. (1990) Surface uplift, uplift of rocks, and exhumation of rocks. *Geology*, **18**, 1173–1177.

Epard, J.-l. & Groshong, R.H., Jr. (1993) Excess area and depth to detachment. *Bull. Am. Ass. petrol. Geol.*, **77**, 1291–1302.

Gallagher, K. (1989) An examination of some uncertainties associated with estimates of sedimentation rates and tectonic subsidence. *Basin Res.*, **2**, 97–114.

Grantz, A. & May, S.D. (1982) Rifting history and structural development the continental margin north of Alaska. In: *Studies in Continental Margin Geology* (Ed. by J. S. Watkins and C. L. Drake), *Mem. Am. Ass. petrol. Geol.*, **34**, 77–100.

Gregory, K. (1994) Palaeoclimate and palaeoelevation of the 35 Ma Florrisant flora, Front Range, Colorado. *Palaeoclim.*, **1**, 23–57.

Guidish, T.M., Kendall, C.G.S.C., Lerche, I., Toth, D.J. & Yarzab, R.F. (1985) Basin evaluation using burial history calculations: An overview. *Bull. Am. Ass. petro. Geol.*, **69**, 92–105.

Hardy, S. & Poblet, J. (1994) Geometric and numerical model of progressive limb rotation in detachment folds. *Geology*, **22**, 371–374.

Heller, P.L. & Paola, C. (1989) The paradox of Lower Cretaceous gravels and the initiation of thrusting in the Sevier orogenic belt, United States Western Interior. *Bull. geol. Soc. Am.*, **101**, 864–875.

Homza, T.X. & Wallace, W.K. (1995) Geometric and kinematic models for detachment folds with fixed and variable detachment depths. *J. Struct. Geol.*, **17**, 575–588.

Jamison, W.R. (1992) Stress controls on fold thrust style. In: *Thrust Tectonics* (Ed. by K. R. McClay), pp. 155–164. Chapman and Hall, London.

Keller, E.A., Johnson, D.L., Laduzinsky, D.M., Rockwell, T.K., Seaver, D.B., Zepeda, R.L. & Zhao, X. (1989) *Tectonic Geomorphology and Late Pleistocene Soil Chronology of the Wheeler Ridge, San Emigdio Mountains and Frazier Mountain Areas*. Guidebook for Friends of the Pleistocene Field Trip.

Kelley, J.S. & Foland, R.L. (1987) Structural style and framework geology of the coastal plain and adjacent Brooks Range. In: *Petroleum Geology of the Northern Part of the Arctic National Wildlife Refuge, Northern Alaska* (Ed. by K. J. Bird and L. B. Magoon), *Bull. US geol. Surv.*, **1778**, 255–270.

Lawton, T.F., Boyer, S.E. & Schmitt, J.G. (1994) Influence of inherited taper on structural variability and conglomerate distribution, Cordilleran fold and thrust belt, western United States. *Geology*, **22**, 339–342.

McRae, L.E. (1990) Paleomagnetic isochrons, unsteadiness, and non-uniformity of sedimentation in Miocene fluvial strata of the Siwalik Group, northern Pakistan. *J. Geol.*, **98**, 433–456.

Medwedeff, D.A. (1989) Growth fault-bend folding at southeast Lost Hills, San Joaquin Valley, California. *Bull. Am. Ass. petrol. Geol.*, **73**, 54–67.

Medwedeff, D.A. (1992) Geometry and kinematics of an active, laterally propagating wedge thrust, Wheeler Ridge, California. In: *Structural Geology of Fold and Thrust Belts* (Ed. by S. Mitra and G. W. Fisher), pp. 3–28. Johns Hopkins University Press, Baltimore.

Meghraoui, M., Jaegy, R., Lammali, K. & Albarede, F. (1988) Late Holocene earthquake sequences on the El Asnam (Algeria) thrust fault. *Earth planet. Sci. Lett.*, **90**, 187–203.

Meigs, A.J. (1990) *Structural Geometry and Sequence in the Eastern Sadlerochit Mountains, Northeastern Brooks Range, Alaska*. Masters thesis, University of Alaska.

Mellere, D. (1993) Thrust-generated, back-fill stacking of alluvial fan sequences, south-central Pyrenees, Spain (La Pobla de Segur conglomerates). In: *Tectonic Controls and Signatures in Sedimentary Successions* (Ed. by L. E. Frostick and R. J. Steel), pp. 259–276. Blackwell Scientific Publications, Oxford.

Molnar, P. & England, P. (1990) Late Cenozoic uplift of mountain ranges and global climatic change: chicken or egg? *Nature*, **346**, 29–34.

Montgomery, D.R. & Dietrich, W.E. (1994) Landscape dissection and drainage area–slope thresholds. In: *Process Models and Theoretical Geomorphology* (Ed. by M. J. Kirkby), pp. 221–246. John Wiley and Sons, New York.

Namson, J. & Davis, T.L. (1988) Seismically active fold and thrust belt in the San Joaquin Valley, central California. *Bull. geol. Soc. Am.*, **100**, 257–273.

O'sullivan, P.B., Green, P.F., Bergman, S.C., Decker, J., Duddy, I.R., Gleadow, A.J.W. & Turner, D.L. (1993) Multiple phases of Tertiary uplift and erosion in the Arctic National Wildlife Refuge, Alaska, revealed by apatite fission track analysis. *Bull. Am. Ass. petrol. Geol.*, **77**, 359–385.

Oberlander, T.M. (1985) Origin of drainage transverse to structures in orogens. In: *Tectonic geomorphology: Proceedings, 15th Annual Binghamton Geomorphology Symposium* (Ed. by M. Morisawa and J. T. Hack), pp. 155–182. Allen and Unwin, Boston.

Ori, G.G. & Friend, P.F. (1984) Sedimentary basins formed and carried piggyback on active thrust sheets. *Geology*, **12**, 475–479.

Riba, O. (1976) Syntectonic unconformities of the Alto Cardener, Spanish Pyrenees: a genetic interpretation. *Sediment. Geol.*, **15**, 213–233.

Roca, E. (1992) *L'estructura de la conca Catalano-Balear: paper de la compressió i de la distensió en la seva gènesi*. PhD dissertation, University of Barcelona, Spain.

Rockwell, T.K., Keller, E.A., Clark, M.N. & Johnson, D.L. (1984) Chronology and rates of faulting of Ventura River terraces, California. *Bull. geol. Soc. Am.*, **95**, 1466–1474.

Rogers, J.A. (1989) Structural Evolution of the central Shublik Mountains and Ignek Valley, northeastern Brooks Range, Alaska. *Alaska Division of Geological and Geophysical Surveys Public Data File 89–1c*, 37.

Russell, B.J. & McMillen, K.J. (1987) Neogene to Quaternary deformation of northeastern Alaska. *Geol. Soc. Am. Abstr. w. Prog.*, **19**, 827.

Sadler, P.M. (1981) Sediment accumulation rates and the completeness of the stratigraphic record. *J. Geol.*, **89**, 569–584.

Scholz, C.G., Dawers, N.H., Yu, J.-Z. & Anders, M.H. (1993) Fault growth and fault scaling laws: preliminary results. *J. geophys. Res.*, **98** (21), 951–21, 961.

Sclater, J.G. & Christie, R.A.F. (1980) Continental stretching: An explanation of the post-mid-Cretaceous subsidence of the central North Sea Basin. *J. geophys. Res.*, **85**, 711–739.

Seeber, L., Armbruster, J.G. & Quittmeyer, R.C. (1981) Seismicity and continental subduction in the Himalayan arc. In: *Zagros Hindu Kush Himalaya Geodynamic Evolution* (Ed. by H. K. Gupta and F. M. Delaney), pp. 215–242. American Geophysical Union, Washington, DC.

Sieh, K., Stuiver, M. & Brillinger, D. (1989) A more precise chronology of earthquakes produced by the San Andreas fault in Southern California. *J. geophys. Res.*, **94,** 603–623.

Suppe, J. (1983) Geometry and kinematics of fault bend folding. *Am. J. Sci.*, **283,** 648–721.

Suppe, J.S., Chou, G.T. & Hook, S.C. (1992) Rates of folding and faulting determined from growth strata. In: *Thrust Tectonics* (Ed. by K. R. McClay), pp. 105–122. Chapman and Hall, London.

Talling, P.J. & Burbank, D.W. (1993) Assessment of uncertainties in magnetostratigraphic dating of sedimentary strata. In: *Applications of Paleomagnetism to Sedimentary Geology* (Ed. by A. Asissaoiu, D. F. McNeil and N. F. Hurley), *Spec. Publ. Soc. econ. Paleont. Miner.*, **49,** 59–69.

Talling, P.J., Lawton, T.F., Burbank, D.W. & Hobbs, R.S. (1995) Evolution of latest Cretaceous-Eocene nonmarine deposystems in the Axhandle piggyback basin of central Utah. *Bull. geol. Soc. Am.*, **107,** 297–315.

Vergés, J. (1993) *Estudi geològic del vessant sud del Pirineu oriental i central. Evolució cinemática en 3D.* PhD thesis, University of Barcelona.

Vergés, J. & Burbank, D.W. (1992) Progressive unconformities: a key to understanding fold-and-thrust evolution. *EOS (Am. Geophys. Un. Trans.)*, **73,** 545–546.

Vergés, J., Burbank, D.W. & Meigs, A. (1996) Unfolding: an inverse approach to fold kinematics. *Geology*, **24**, 175–178.

Wallace, W.K. & Hanks, C.L. (1990) Structural provinces of the northeastern Brooks Range, Arctic National Wildlife Refuge, Alaska. *Bull. Am. Ass. petrol. Geol.*, **76,** 1100–1118.

Willis, B. (1993) Ancient river systems in the Himalayan foredeep, Chinji Village area, northern Pakistan. *Sediment. Geol.*, **88,** 1–76.

Zepeda, R.L., Keller, E.A. & Rockwell, T.K. (1990) Soil chronology and active tectonics at Wheeler Ridge, southern San Joaquin Valley, California. In: *Soils and Landscape Evolution: 21st Annual Binghamton Geomorphology Symposium, Prog. and Abstr.,* p. 41. State University of New York at Binghamton, Binghamton.

Received ?? ???? 1995; revision accepted ?? ???? 1996.